ISSN-1101-9824
ISRN LUTVDG/TVVR–07/5003 72

Seasonal Closure of Chilaw Inlet in Sri Lanka

-Physical Processes and Mathematical Modelling-

Alexandra Angelbratt and Jon Klüft

Supervisors: Magnus Larson[1] and Nalin Wikramanayake[2]

Division of Water Resources Engineering
Department of Building and Environmental Technology
Lund Institute of Technology
Lund University

Lund 2007

Printed in Sweden

[1] Professor, Division of Water Resources Engineering, Lund Institute of Technology
[2] Doctor, Department of Civil Engineering, Open University of Sri Lanka

LUNDS TEKNISKA HÖGSKOLA
Lunds universitet

Lund University
Faculty of Engineering, LTH
Departments of Earth and Water Engineering

This study has been carried out within the framework of the Minor Field Studies (MFS) Scholarship Programme, which is funded by the Swedish International Development Cooperation Agency, Sida.

The MFS Scholarship Programme offers Swedish university students an opportunity to carry out two months' field work in a developing country resulting in a graduation thesis work, a Master's dissertation or a similar in-depth study. These studies are primarily conducted within subject areas that are important from an international development perspective and in a country supported by Swedish international development assistance.

The main purpose of the MFS Programme is to enhance Swedish university students' knowledge and understanding of developing countries and their problems. An MFS should provide the student with initial experience of conditions in such a country. A further purpose is to widen the human resource base for recruitment into international co-operation. Further information can be reached at the following internet address: http://www.tg.lth.se/mfs

The responsibility for the accuracy of the information presented in this MFS report rests entirely with the authors and their supervisors.

Gerhard Barmen
Local MFS Programme Officer

Sammanfattning

Chilaw inlopp med tillhörande lagun är belägen på Sri Lankas västkust cirka 120 km norr om huvudstaden Colombo. Varje år under sommarmonsunen, som varar från maj till september, så stängs inloppet igen till följd av bildningen av en sandsporre ("spit"). Stängningen resulterar i att de fiskare som använder lagunen som ankringsplats för sina båtar inte längre kan nå havet och att vattenkvaliteten i lagunen försämras eftersom det inte sker något vattenutbyte med havet. Teori bakom stängningen av inlopp studerades i föreliggande rapport för att förstå vilka fysiska mekanismer som är kopplade till stängningen av Chilaw inloppet. En fältmätningskampanj utfördes också från maj till och med juli (2006) vilken resulterade i topografikartor beskrivande de morfologiska förändringarna kring inloppet under sommarmonsunen.

En ökad kustparallell sandtransport under sommarmonsunen 2006 och en pålandsriktad sandtransport från en sandrevel, belägen på havssidan av inloppet, gav upphov till en sandsporre som växte till utanför utloppet. I början av juli orsakade sandsporren en stängning av inloppet. I slutet av juli bröts sandsporren itu vilket resulterade i en öppning av inloppet. Öppningen skedde till följd av minskad kustnära sandtransport och hög vågenergi mot sandsporren.

Utifrån vågdata och strandtopografin skapades två matematiska modeller, en enkel och en mer avancerad. De olika sedimentflödena vid inloppet identifierades och kvantifierades, och med hjälp av en reservoirmodell modellerades utvecklingen av sandsporren. Båda modellerna visade sig kunna beskriva den observerade tillväxten tillfredsställande, men eftersom den avancerade modellen innehåller fler antaganden och kräver mer värden på koefficienter bedöms den enkla modellen vara mest pålitlig och användbara med tanke på befintlig data. För att erhålla ett bättre resultat med den avancerade modellen krävs att fler fysiska processer vid inloppet mäts och kvantifieras.

Abstract

Chilaw inlet, with the affiliated lagoon, is located on the west coast of Sri Lanka about 120 km north of the capital Colombo. Each year during the summer monsoon, which lasts from May to September, the inlet closes due to a sand spit forming across the inlet. The closure results in impeded access to the sea for the fishermen, who use the lagoon as anchorage for their boats, and in deteriorated water quality in the lagoon. The theory behind inlet closure was studied in the present investigation in order to understand the governing physical mechanisms related to closure at Chilaw inlet. A measurement campaign, lasting from May to July (2006), was also performed resulting in topographic maps describing the morphological changes at the inlet during the summer monsoon.

Increased longshore sediment transport during the summer monsoon 2006 and cross-shore sediment transport from an ebb shoal, located seaward of the inlet, initiated spit formation, which by early July led to an inlet closure. By the end of July a breaching of the spit occurred due to a combination of decreased longshore sediment transport and large amounts of wave energy working on the spit.

Based on wave data and topographic maps two mathematical models were developed, one basic and one more advanced. The sediment pathways at the inlet were identified and quantified, and through a reservoir-type model the spit growth was simulated at the inlet. Both models described the observed spit growth fairly well but, since the advanced model involves more assumptions and coefficients than the basic model, the latter on is judged to be the most reliable and suitable with regard to the data available. In order to obtain a better result with the advanced model more physical processes have to be measured and quantified.

Keywords

Tidal inlets, Chilaw inlet, Spit Evolution, Sediment Transport, Inlet Closure, Mathematical Model

Preface

While looking for a master thesis we heard that a project was going on in Sri Lanka and when we got a little more information about it we decided to apply. We got a scholarship from the Swedish aid organization SIDA for a Minor Field Study and in the beginning of June 2006 we went to Sri Lanka for a two-month stay. Everything did not go as planned but in the end we can only say that it has been a rewarding and fun experience. This report is based on data from the field measurements that were undertaken during the summer of 2006 in Sri Lanka and from wave data from 1995-1997.

We would like to thank our supervisors, Professor Magnus Larson and Dr. Nalin Wikramanayake, who helped us with this master thesis. Nalin Wikramanayake made the Chilaw field measurements possible and provided knowledge about the study area. Magnus Larson gave us valuable input during the mathematical modelling and reviewed the master thesis and gave many helpful suggestions.

We also wish to thank Upul and his family who welcomed us in their home in Colombo.

Table of Contents

Introduction

Background

A coastal inlet is an opening through a landmass which, via a waterway, connects the ocean with a body of water, such as a lagoon or bay (Kraus, 2002). In parts of the world, for example, Australia and Sri Lanka, inlets are seasonally closed due to sediment transport. Typical features of the seasonally closed inlets are that they occur in micro- tidal, wave-dominated coastal environments where the seasonal stream flow and wave climate variations are large (Ranasinghe and Pattiaratchi, 1997).

The Chilaw estuary is located on the west coast of Sri Lanka about 120 km north of the capital Colombo, see Figure 1. Figure 1 also shows the Chilaw lagoon system including the lagoon, the 5 km long entrance channel, which connects the lagoon with the estuary and ocean, and the mouth of the Deduru River. A sandstone reef stretches for about 5.5 km in a southern direction along the coast from the inlet. Chilaw inlet is located in a micro-tidal area and every year during the south-west monsoon, approximately from May to September, a spit is formed across the inlet and causes a closure (Wikramanayake and Pattiaratchi, 1999).

The main industry in Chilaw is fishing and the lagoon and the entrance channel are used as anchorage by a large fleet of fishing boats; around 7000 fishing boats pass through the inlet every day (Baranasuriya, 2001; Ranasinghe and Pattiaratchi, 1997). When the inlet closes during the south-west monsoon the access to the ocean becomes restricted which leads to large negative consequences for the Chilaw fishing industry. The inlet is typically opened artificially in order to gain access to the ocean for the fishing fleet (Wikramanayake and Pattiaratchi, 1999). Another problem related to the closure of an inlet is the deterioration of the water quality in the lagoon and estuary (Ranasinghe et al., 1999).

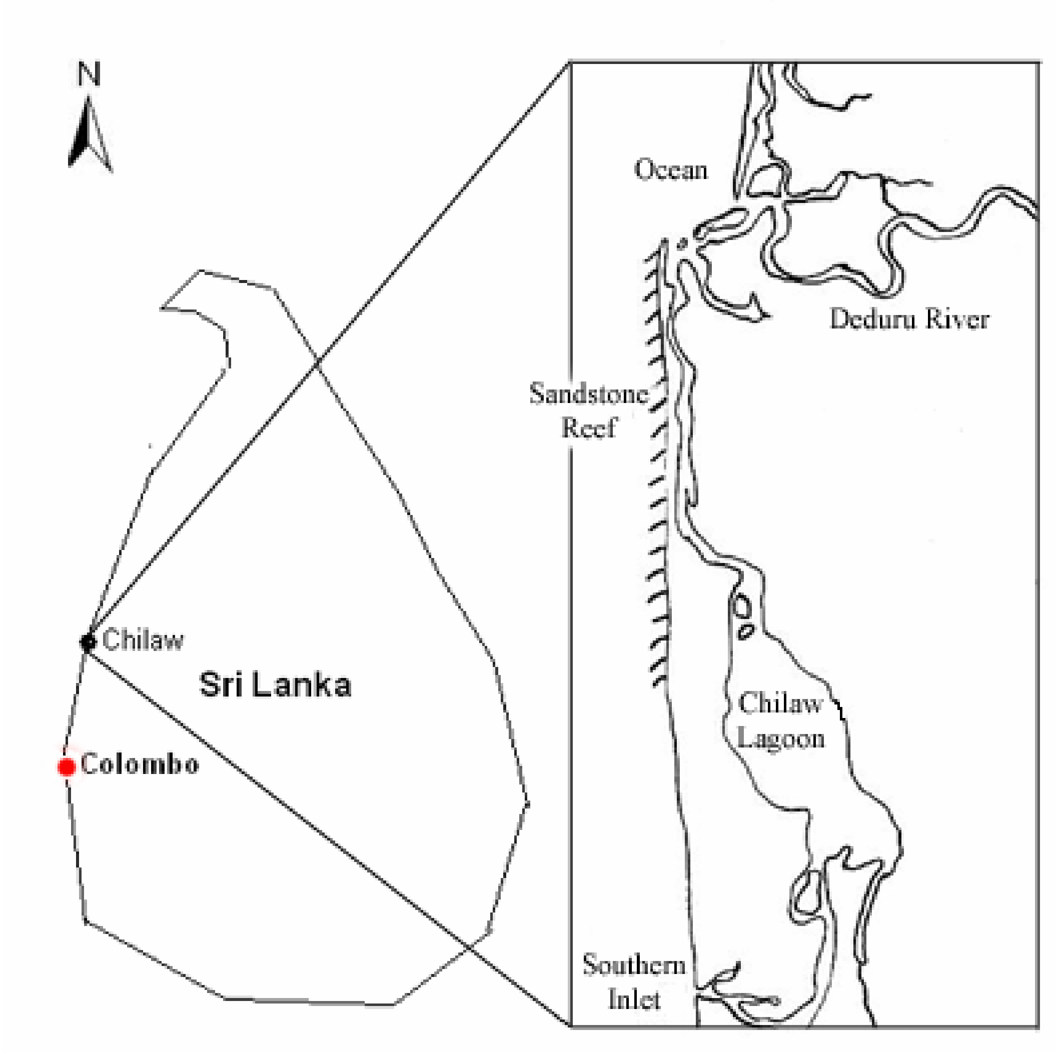

Figure 1: Sri Lanka and the Chilaw study area

Objectives and Procedure

The three main objectives of this master thesis are: (1) to gain an increased understanding about seasonally closed tidal inlets, (2) to measure and analyze the spit formation at Chilaw during the south-west monsoon, (3) and to develop a mathematical spit growth model. Further descriptions of the objectives and how they will be fulfilled are as follows:

- Gain increased knowledge about tidal inlets in general and Chilaw inlet in particular which will be done through a literature study. Special focus will be on the mechanisms behind tidal inlet closure. The aim is to apply these mechanisms when analyzing the morphological change and developing the mathematical model.

- Measure the morphological changes and collect data during the inlet closure period at Chilaw inlet. Observe and try to understand the physical processes that control sediment transport and morphological change during the south-west monsoon. The measurement campaign will result in morphological maps covering the inlet closure caused by the spit growth.

- Build a basic mathematical model describing the spit growth. The model will be applied and compared with the characteristic length of the spit, obtained from the morphological maps during the field measurements.

Report Structure

The report is divided into five major parts: Physical Processes at Tidal Inlets, Study Area Chilaw, Field Measurements, Analysis of Field Data, and Inlet Response Modelling.

In the first part general theory and common processes at tidal inlets are presented. Then, the physical setting at Chilaw, and the measurement campaign and analysis of field data including the construction of morphological maps are discussed. Finally a mathematical model of different scenarios concerning the change in spit morphology is developed using MATLAB.

Physical Processes at Tidal Inlets

The general morphology of tidal inlets and background theory for the mechanisms governing inlet closure and opening are presented in this chapter.

Inlet Morphology

The principal depositional sand morphology units associated with tidal inlet are the tidal deltas and the recurved spit. The spit is related with the inlet migration which may cause an inlet closure. Inlet morphology is depending on the ratio of wave energy to tidal current energy, the volume of the tidal prism, the size of the back barrier area, and the difference in ebb and flood-tide velocity (Hayes, 1980). Hayes (1980) proposed the terminology ebb-tidal delta and flood-tidal delta. Engineers generally use the words ebb shoal and flood-shoal, see Figure 2, and in the report this terminology is used. According to Hayes (1980) both the ebb shoal and flood-shoal usually contains typical morphological components, however these are not of great interest in the Chilaw study and will therefore not be described further.

The ebb shoal is a sediment accumulation seaward of the inlet. Large ebb shoals and small flood shoals generally develop in areas with large tides and small waves (Hayes, 1980). The deposition is mainly caused by ebb currents and sediment is transported offshore by the ebb current in the main ebb channel located in the middle of the inlet. Since the velocity decreases further away from the inlet the sediment finally deposits. The small waves usually modify the size and shape of the ebb shoal (Hayes, 1980).

The flood shoal is a sediment accumulation formed on the landward side of the inlet. Areas with small tides and large waves contribute to a dominant flood-tidal current (Hayes, 1980). The result is usually a sediment transport to the landward side of the inlet where the sediment is deposited and forms a flood shoal. Areas with small tides and large waves usually create large flood-shoals and small ebb shoals, due to the fact that large waves often inhibit development of ebb shoals (Hayes, 1980).

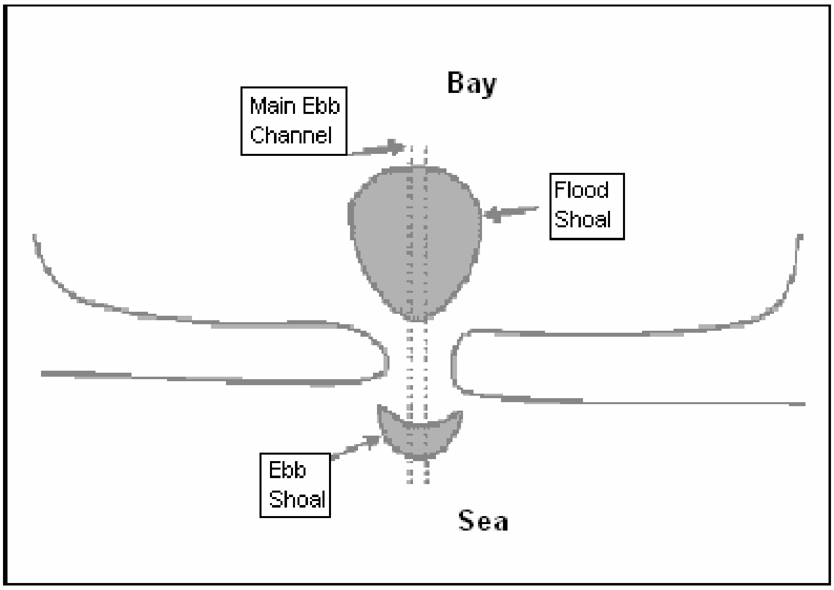

Figure 2: Definition sketch of inlet morphology

Beach and Wave Nomenclature

Some of the general beach and wave nomenclature used in this study are shown in Figure 3 and Figure 4. Offshore is the flat portion of the beach profile which extends seaward from the near shore zone. The breaker zone is the part of the nearshore region where the waves arriving from the offshore breaks. In the surf zone bore-like waves occur following wave breaking and the swash zone represents the part where the beach face is alternately covered by the runup of the wave uprush and exposed by the backwash.

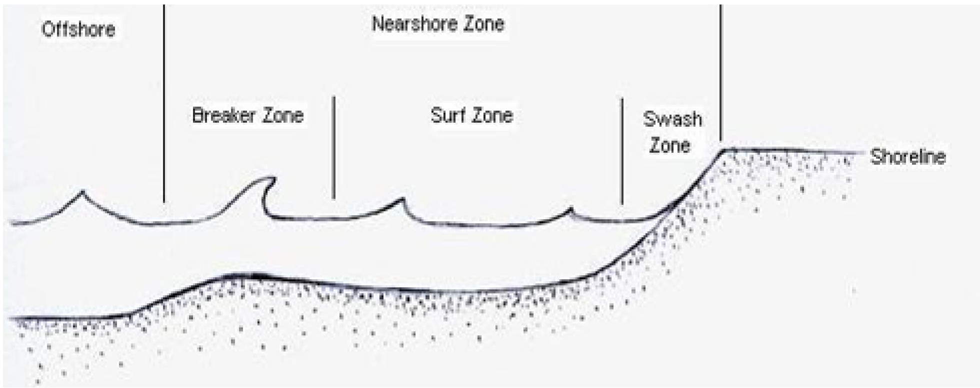

Figure 3: Definition of different zones across a beach profile with respect to wave dynamics (after Komar, 1998)

In Figure 4 the different morphodynamical elements of a beach profile are presented. The offshore is the same as in Figure 3 and foreshore, often referred to as beach face, is the part lying between the upper limit of wave uprush and the low water mark. The inshore zone is situated between the offshore and the foreshore zone. A longshore bar is an underwater ridge of sand running parallel (approximately) to the shoreline. Often, several bars can be observed parallel to each other but at different depths. A longshore trough is an elongated depression extending parallel to the shoreline. Several troughs can be present along a beach and they are always occurring on the shoreward side of a longshore bar. The backshore zone is the part of the beach behind the foreshore which extends landward until there is a shift in physiography.

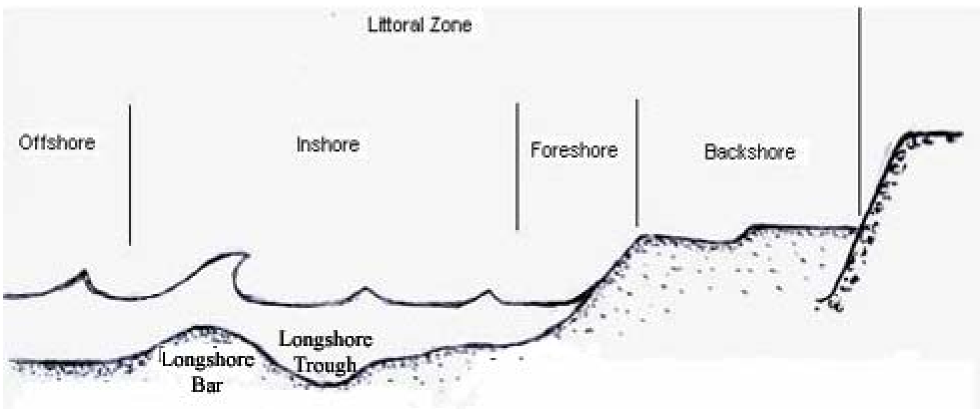

Figure 4: Definition of different features and zones across a beach profile with respect to morphodynamics (after Komar, 1998)

Wave Transformation

According to Komar (1998) two types of waves can be distinguished, that is sea and swell waves. Sea waves arise in storm areas and have the whole spectrum of periods and heights, whereas swell waves have more uniform heights and distances between the crests. Swell waves can be followed from a storm area and for a long travel distance. Within the swell waves energy may be transported across the oceans and delivered to the coastal zones. When a wave reaches a coastal region, such as an inlet, it changes character due to changes in bathymetry and/or disturbance by obstacles. Common phenomena that occur are wave breaking, shoaling, refraction, and diffraction (Komar, 1998).

Wave Breaking and Shoaling

When a wave encounters shallow water it undergoes a transformation. The wavelength and velocity decreases while the height increases and the wave period remains constant. Immediately seaward of the breaker zone, the waves consist of peaked crests separated by flat troughs. When the waves reach a certain height with respect to the water depth (or wavelength in deep water) they become over-steepened, which results in instability and subsequent breaking. The transformation is most significant for long-period swell waves since they are lower than locally formed sea waves, which are initially higher even in deep water (Komar, 1998).

Wave Refraction

Different physical factors, such as bathymetry or currents, may change the movement and direction of the waves. When a wave encounters shallower water at an angle to the underwater contours the part of the wave which is in deeper water will move faster, while the part in the shallow water will decrease its speed (US Army Corps of Engineering, 1984). This will cause a bend of the wave crest which is called refraction and is the same phenomenon as light refraction. For straight coastlines with parallel bathymetric contours the waves tend to become parallel with the contour line. Divergence or convergence of wave energy can arise due to irregular bottom contours, for example, a submarine canyon will cause the waves to diverge according to the previous discussion (US Army Corps of Engineering, 1984). An example of wave convergence occurs over a submarine headland or at the sides of a submarine canyon. Divergence will produce lower waves with less energy, whereas convergence will cause the opposite (Komar, 1998). An increased understanding of wave refraction will facilitate predictions concerning the wave energy distribution along a coast, which in turn can give insight to where erosion and deposition will occur. Refraction contributes to changes in the bathymetry because it affects erosion and deposition of beach sediment (US Army Corps of Engineering, 1984). According to US Army Corps of Engineering (1984) there is a relationship between refraction, wave energy distribution along a shore, and the erosion/deposition of beach materials. Through studies of wave pattern near the beach from, for example, aerial photographs, it is possible to get a general understanding of the underlying bathymetry.

Wave Diffraction

Diffraction of waves, which is often occurring in combination with refraction, is when energy is transferred laterally along a wave crest from points of higher to lower wave height (US Army Corps of Engineering, 2006). When a barrier, such as a breakwater for sheltering harbors obstructs the wave propagation a calm zone behind the breakwater appears (shadow zone). However, wave energy tends to leak into the shadow zone that may create undesirable wave conditions in the harbor through the phenomenon of wave diffraction (Komar, 1998).

Sediment Transport

There are different types of sediment transport but the ones of greatest importance when studying tidal inlet closure is longshore and cross-shore sediment transport (Komar, 1998).

Longshore Sediment Transport

Longshore sediment transport denotes beach sediment transported by waves and currents along the coast in the nearshore zone. The wave approaches the coast at an angle and creates a shore-parallel current that carries sediments further along the coast (Komar, 1998; US Army Corps of Engineering, 2006). The transport causes sediment displacement at various scales from local movement in bars and troughs to large sediment movement along the coast (Komar, 1998; US Army Corps of Engineering, 2006). A (natural) tidal inlet interrupts the longshore sediment transport and sediment is accumulated at the updrift side of the inlet and in most cases also at the down-drift side (Ranasinghe et al., 1999). In many cases inlets have been stabilized using jetties, which tend to enhance the accumulation on the updrift side and cause marked erosion on the downdrift side. The interaction between the longshore sediment transport and the transport in the tidal flow may give rise to a number of morphological features, such as the ebb and flood shoals previously discussed. Also, whether the inlet closes depends on the interaction between the longshore sediment transport and the inlet clearing mechanisms such as tides and waves (Ranasinghe et al., 1999). The along-coast movement is also referred to as littoral sediment transport, whereas the actual sediment volume that is displaced is called the littoral drift (Komar, 1998; US Army Corps of Engineering, 2006).

Cross-Shore Sediment Transport

Cross-shore sediment transport denotes the sediment movement perpendicular to the coast and includes both offshore and onshore transport. Offshore transport occurs during higher wave conditions such as storms, while onshore transport occurs during mild wave conditions (Komar, 1998; US Army Corps of Engineering, 2006). During offshore transport the beach face is exposed to erosion and its size decreases, and the eroded sediment is deposited offshore as a longshore bar or shoal. During onshore transport packets of sand moves towards shore and connects to the beach. In this case erosion takes place in the offshore areas. The onshore movement of sediment contributes to inlet closure, if the clearing mechanisms are weak compared to the sediment transported onshore (Ranasinghe et al., 1999).

Natural Sediment Bypassing

Natural inlet bypassing is when sediment is transported by the waves and currents from the updrift side of an inlet to the down-drift side. This process is the result of interaction between the longshore transport and inlet currents which force the sediment around the edge of the ebb shoal promoting stability of the down-drift shore line (Dean, 1988). Inlet bypassing through persistent sediment transport along the ebb shoal is called continuous bypassing (Dean, 1988). There is also discontinuous bypassing and FitzGerald (1988) describes three examples of this type involving bypassing of large packets of sediment: stable inlet processes, ebb-tidal delta breaching, and inlet migration and spit breaching.

Stable Inlet Processes

A stable inlet should have a main ebb channel that does not migrate and a stable inlet throat position. At those kinds of inlet sand bypassing can occur. Swash bars, which forms in the distal part of the ebb shoal of sand transported in the ebb channel, lump together and form a large bar complex that migrate landward to the down drift shoreline. The reason for this is the dominance of net landward flow in the swash zone since during flood the current gets reinforced by the swell waves and during ebb the ebb current gets retarded by the swell waves.

Ebb-Tidal Delta Breaching

Ebb-tidal delta or ebb-shoal breaching is the process when sand is bypassed through migration of the main ebb channel. The longshore sediment transport causes a sediment buildup on the updrift side of the inlet which deflects the ebb channel. This process can go on until the main ebb channel runs almost parallel with the down drift shoreline and it causes significant erosion. It is not efficient for the water to flow this way so gradually, or during a single storm event, the flow will be diverted and start to flow over the sand accumulation and finally break the tidal delta. The former channel will be filled with sediment due to decreased water flow through it and soon all the water will go through the new channel. The rest of the delta forms a large bar complex which, through onshore movement, migrates to the down-drift beach. Ebb-tidal delta breaching results in bypassing of a lot of sediment from the up drift to the down-drift side of the inlet.

Inlet Migration and Spit Breaching

Sediment from longshore transport adds mostly to the updrift side of an inlet (natural), which decreases the inlets flow area. In order to maintain its discharge the current velocity increases and erodes the down-drift side of the inlet. The result is a migrating inlet, where the migration is dependent of many factors such as wave energy, tidal current, and channel bank composition. Shallow inlets migrate more easily than deeper ones. This is because the shallow channels most likely have eroded only to the barrier sand and the deep ones down to semi-consolidated materials. Sometimes the migration of tidal inlets results in an elongation of the inlet channel which in turn will make the tidal flow between the ocean and the bay ineffective. If a storm occurs the developed spit might breach and a new inlet will be created with a shorter inlet channel. Spit breaching is facilitated if the barrier that separates the channel from the sea is eroded. Bypassing of sand from the updrift side of the inlet to the down-drift side is the result of spit breaching.

Tidal Inlet Closure

There are two main mechanisms for inlet closure presented by Ranasinghe et al. (1999):

The first mechanism is based on the interaction between the longshore current and the inlet current. When the longshore current is interrupted by the tidal current sediment will be deposited on the updrift side of the inlet and form a shoal. If the longshore transport is persistent the shoal will grow and finally a spit may emerge. A smaller shoal may also develop on the down-drift side of the inlet. This shoal is formed by sand sedimentation when the ebb current is retarded and shifted towards the down-drift side of the inlet by the longshore current. If the inlet current is weak compared to the longshore current the spit will continue to grow until it blocks the whole inlet. This type of process is likely to happen in areas with large longshore sediment transport and straight beaches.

The second mechanism occurs when the inlet current is weak, smaller than 1 m/s. Interaction between the inlet current and the onshore sediment transport, when the longshore sediment transport is small, is dominant. Under a storm event sand from the dry beach and the surf zone is transported offshore and forms a longshore bar where the waves are breaking. After the storm, long-period swell waves starts to dominate, and the wave forces the sand stored in the offshore bar to migrate landwards. If the inlet ebb current is strong it can counteract the landward migration, especially in areas close to the inlet, but if the inlet current is weak the inlet will be closed.

It is of great importance to find the dominant mechanism when studying inlet closure. For example in the case of Mvoti estuary in South Africa it may first look like closure is caused by spit growing in the alongshore direction with the longshore transport as the main driving force (Cooper, 1993). In fact, it is an onshore movement of a submerged shoal that causes the inlet closure (Cooper, 1993). In some cases, like Chilaw inlet, interactions between both mechanisms are likely to cause the inlet closure (Wikramanayake and Pattiaratchi, 1999).

Study Area Chilaw

Climate

The climate of Sri Lanka is tropical with dry and wet seasons, including two monsoons. Yala monsoon, which last from May to September, affects the south-western part of the country, while the Maha monsoon blows from December to February over the north and eastern part of the island (Plunkett and Ellemor, 2003). In between the monsoons there are dry periods but in the south-western parts of Sri Lanka, the wet zone, rainfalls are abundant all of the year. In the northern and eastern parts of the country the dry periods are more pronounced and this area is subsequently called the dry zone. The wet zone comprises about 15,000 km^2 and the dry zone 50,000 km^2 (Domroes and Ranatunge, 1993) and every year the zones receive up to 4000 mm and 1000 mm rain respectively (Plunkett and Ellemor, 2003). In 2006, during which the present field measurements were carried out, the Yala monsoon, which affects the Chilaw area, started around the 22nd of May (Department of Meteorology – Sri Lanka, 2006).

Due to large differences in altitude, from the low-lying coastal regions to the hill country with altitudes larger than 1500 m, the temperatures vary significantly (Plunkett and Ellemor, 2003). The average temperature of Colombo is 27˚C, whereas it is only 16˚C at Nuwara Eliya situated in the hill country at an altitude of 1900 m (Plunkett and Ellemor, 2003).

Tide and Wave Climate

Chilaw is located in a micro-tidal region (Wikramanayake and Pattiaratchi, 1999), that is, the difference between the highest and lowest water level, (i.e., the tidal range) does not exceed 2 meters (Komar, 1998). The maximum tidal range in the Chilaw estuary is 0.75 m and occurs during the spring tide. Furthermore, the lagoon entrance channel has a maximum ebb discharge of 178 m^3/s and a tidal prism of 2.4 Mm^3 (Wikramanayake and Pattiaratchi, 1999). The tidal prism is defined as the volume of water exchanged between an estuary or lagoon and the open sea during one tidal period.

When the south-west monsoon starts the sea waves change direction, from about 220 degrees to 255 degrees related to true north (Wikramanayake and Pattiaratchi, 1999). Approximately 60 percent of the sea waves exceed the height of 1 meter throughout the monsoon and the direction of the swell waves is 240 degrees with a wave height of 0.6 m in average (Wikramanayake and Pattiaratchi, 1999).

Physical Setting

The layout of the Chilaw study area is presented in Figure 1. The lagoon area is about 500 ha and the surrounding land use is mostly dominated by prawn cultivation, coconut plantations, and marsh land (Survey Department of Sri Lanka, 2000; Wikramanayake and Pattiaratchi, 1999). There are two connections between the lagoon and the sea, one in the south, the south inlet, which is open only for a couple of weeks during the peak of the rainy season, and one in the north, which is reached by the lagoon channel (Wikramanayake and Pattiaratchi, 1999). The northern estuary is divided into three inlets. The main inlet is located to the west, the north-east inlet is located where the Deduru River flows into the sea, and a small inlet is located in between the main and Deduru inlet. Deduru River is located to the north of the lagoon channel entrance and meanders in an eastern direction for about 9 km before it changes direction (Survey Department of Sri Lanka, 2000).

Inlet Morphology

Figure 5 shows the Chilaw inlet and its main morphological elements during the south-west monsoon. The western coast is defined by the sandstone reef covered by a dune. At the northern end of the reef sand is accumulated, which induces a spit growth across the inlet towards the east. An ebb shoal is situated just seaward of the inlet. The entrance channel that passes between the spit and the barrier island leads to the Chilaw lagoon.

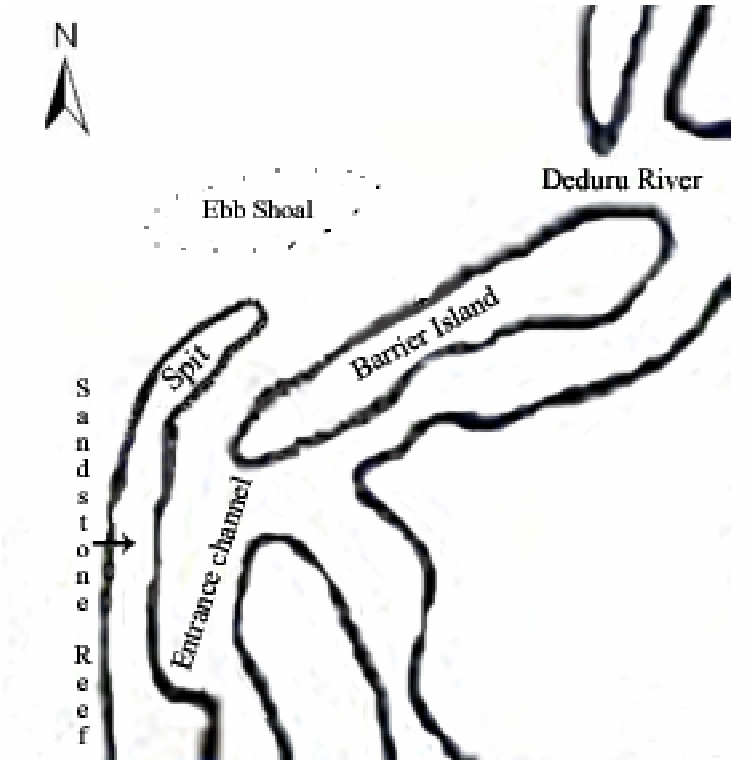

Figure 5: Typical Chilaw inlet morphology

Ebb Shoal

Since Chilaw inlet is located in a micro-tidal area it should, according to Hayes (1980), include a small ebb shoal and a large flood shoal, but this is not the case. No flood shoal features can be seen inside the inlet and according to Wikramanayake and Pattiaratchi (1999) there are no signs of increased sediment masses in the lagoon since 1956. An ebb shoal is present, however, as seen in aerial Photos from Lanka Hydraulic Institute (1998) that shows brighter parts beneath the water surface in August 1995, seaward of the inlet, clearly indicating sand accumulation in an ebb shoal. A similar discussion is also presented in the Lanka Hydraulic Institute Report (1998). According to Hayes (1980) could the presence of high waves, such as the ones from the south-west monsoon, inhibit the formation of an ebb shoal. However, since the sandstone reef protects the inlet from the dominant south-west monsoon waves it is possible that an ebb shoal forms.

Sandstone Reef

Figure 6 shows the sandstone reef, which can be seen to the left in the photo where the waves break, and the sand dune that covers the reef. The sandstone reef stretches for about 5.5 km in a North-South direction and separates the inlet channel from the ocean, to the left in the picture. The width of the reef varies from 50 - 150 meters and the extent is from between 1.5 - 4 m below mean sea level, MSL, to 0.25 - 0.75 m above MSL (Wikramanayake and Pattiaratchi, 1999). Along all of the coast line the reef is more or less vertical. At the northern end, the reef is mainly below sea level, 0.5 – 1 m, for about 150 meters and then it suddenly ends (Wikramanayake and Pattiaratchi, 1999). On top of the reef lies a sand dune which varies in height along the reef.

Figure 6: The northern part of the sandstone reef covered by the sand dune

Barrier Island

According to Komar (1998) the definition of a barrier island is "an unconsolidated elongate body of sand or gravel lying above the high-tide level and separated from the mainland by a lagoon or marsh."

In Chilaw one main barrier island, which sometimes is breached into two, is located in the middle of the estuary, see Figure 5 (Wikramanayake and Pattiaratchi, 1999). It stretches for about 1200 m in a south-west north-east direction. The width of the barrier island varies significantly, from a couple of meters, where the breaching will occur, to about 240 meters at its widest point (Wikramanayake and Pattiaratchi, 1999).

Deduru River

The largest part of Deduru river catchment area is located where mainly the rain falls during the north-east (Maha) monsoon and therefore, the river flow is small during the south-west monsoon (Ranasinghe and Pattiaratchi, 1997). Calculations show that 90 percent of the sedimentation in the estuary caused by the river flow occurs over one week during the months of October and November (Wikramanayake and Pattiaratchi, 1999). Because of this the Deduru river will not be taken into account when discussing Chilaw inlet closure in this study.

Inlet Closure

When the monsoon starts in May the winds shift to a more westerly direction and this change in wind conditions initiates a longshore sediment transport to the north from areas further south of the sandstone reef. When the sediment reaches Chilaw inlet the longshore current will be interrupted and the sediment stream is divided into two pathways at the top of the sandstone reef (Wikramanayake and Pattiaratchi, 1999). Waves will force the sediment around the tip of the sandstone reef and initiate a growth of the sand spit across the inlet. Some of the sediment transport will go seaward and deposit on the ebb shoal. Wave refraction, breaking, and diffraction will occur at the inlet due to the ebb shoal and the sheltering sandstone reef. The waves cause onshore movement of sand from the ebb shoal to the spit. A combination of the onshore movement and spit growth causes the inlet closure at Chilaw (Wikramanayake and Pattiaratchi, 1999).

Field Measurements

Experimental Setup and Procedure

The field work started on the 20th of May and continued until the 30th of July 2006 with a total of nine field days. In the beginning the aim was to undertake measurements every week but due to, among other things, risk of mines and time restrictions, data are missing for some weeks. The field work consisted of measuring the spit, sand bar, and part of the barrier island regarding the elevation using a specially defined coordinate system, see Figure 7. Two different measurement methods were used, that is, measurements with a leveling instrument and with a total station.

When using the leveling instrument a cross-section approach was employed. The cross sections were measured every 20 meter, orthogonal to a line from one fixed point to another fixed or temporary point always starting in point A or B, Figure 7. Measurements were taken along the orthogonal line at every position where a clear topographic change was observed. The temporary points were located on the spit and on the western side of the barrier island. These points had to be changed each measurement week due to the morphological change in the area. Figure 7 shows the fixed point positions, which were not affected by the morphological changes. By using the total station and two of the fixed points, positions for the temporary points were determined each week.

By using a total station, which measured position and elevation in a differently defined coordinate system, easy analyzed data were obtained. During the campaign the measurement instrument was calibrated to point D and E, Figure 7. The two different coordinate systems were later connected and the data sets for each week were compiled. The elevation relationship between the stationary points A and B were determined by leveling to make adjustment of all the data to the mean sea level possible. A sketch of the area was also made every week to visualize the morphological changes. These sketches were used for comparison with the resulting data plots and in the morphological change discussion.

Seven of the nine field days proved to have sufficient data for further detailed analysis, namely the dates 060528, 060611, 060702, 060708, 060715, 060723, and 060730 (year, month, day).

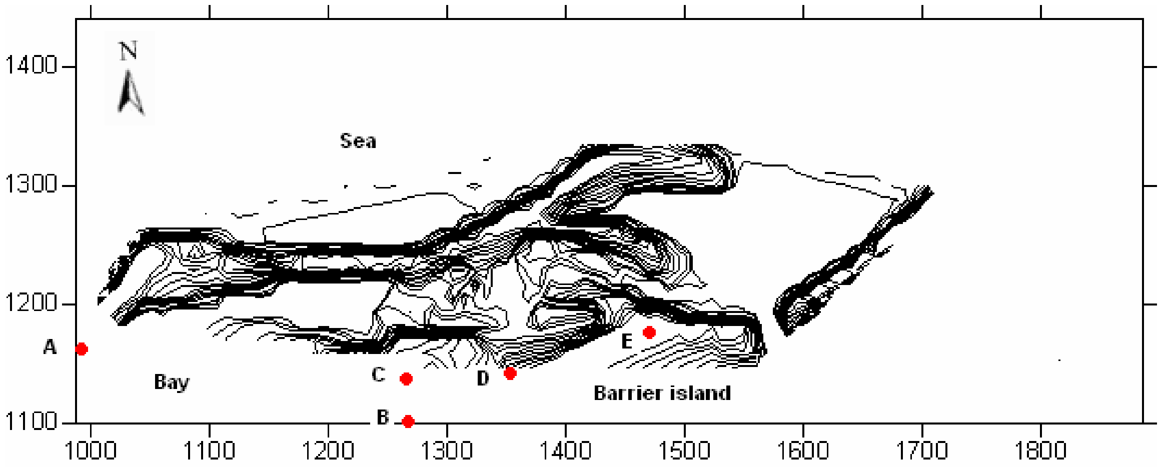

Figure 7: Specially defined coordinate system with stationary points in the measurement area

Analysis of Field Data

Limitations during Field Work

Different problems, expected and not expected, occasionally made it difficult to obtain data of sufficient quality and this is important to have in mind when interpreting the results, both in morphological change analysis and the model simulations. The main issues are listed below:

- As previously mentioned the political situation in Sri Lanka was not stable so there were no measurements on Sunday the 18th of June due to risk of mines planted by the Liberation Tigers of Tamil Eelam, LTTE (ITN, 2006).

- Language difficulties sometimes made it hard to communicate which led to occasional misunderstandings between the participants in the field measurements.

- It happened that the blocks that indicated the stationary points were moved from one week to another. This made it difficult to obtain accurate data concerning position and elevation of the points.

- Finally, the authors felt a bit lost in a foreign country.

Data Entry and Processing

All the field data were entered and processed in Excel. Construction of morphological contour plots and calculation of spit areas and volumes was done in Golden Software Surfer 8.

Overview of Morphological Change

An overview of the changes in morphology during the measurement campaign is presented in Figure 8a-g and discussed in this chapter. When studying the plots it is important to know that for the different field days the same area was not always measured, which introduces some difficulties when comparing the different morphological features from one day to another. Another aspect to keep in mind is that the plots are not always an exact representation of the topography since interpolation was carried out in Surfer. When discussing the maps, information from the sketches that were made during each field day, photographs, and personal observations were also taken into account.

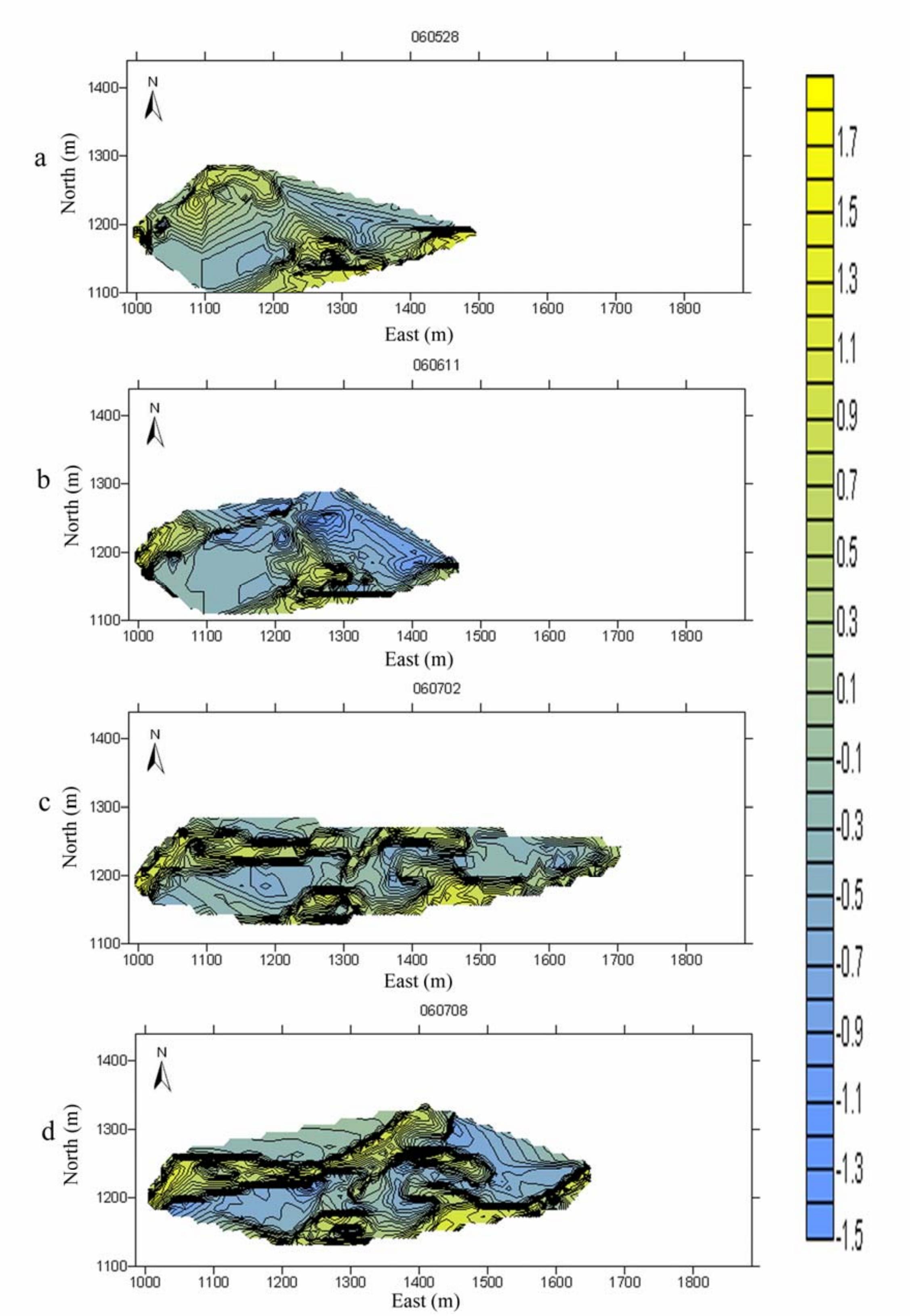
060528
a
North (m)
East (m)
060611
b
North (m)
East (m)
060702
c
North (m)
East (m)
060708
d
North (m)
East (m)
1400
1300
1200
1100
1000
1100
1200
1300
1400
1500
1600
1700
1800
N
1.7
1.5
1.3
1.1
0.9
0.7
0.5
0.3
0.1
-0.1
-0.3
-0.5
-0.7
-0.9
-1.1
-1.3
-1.5

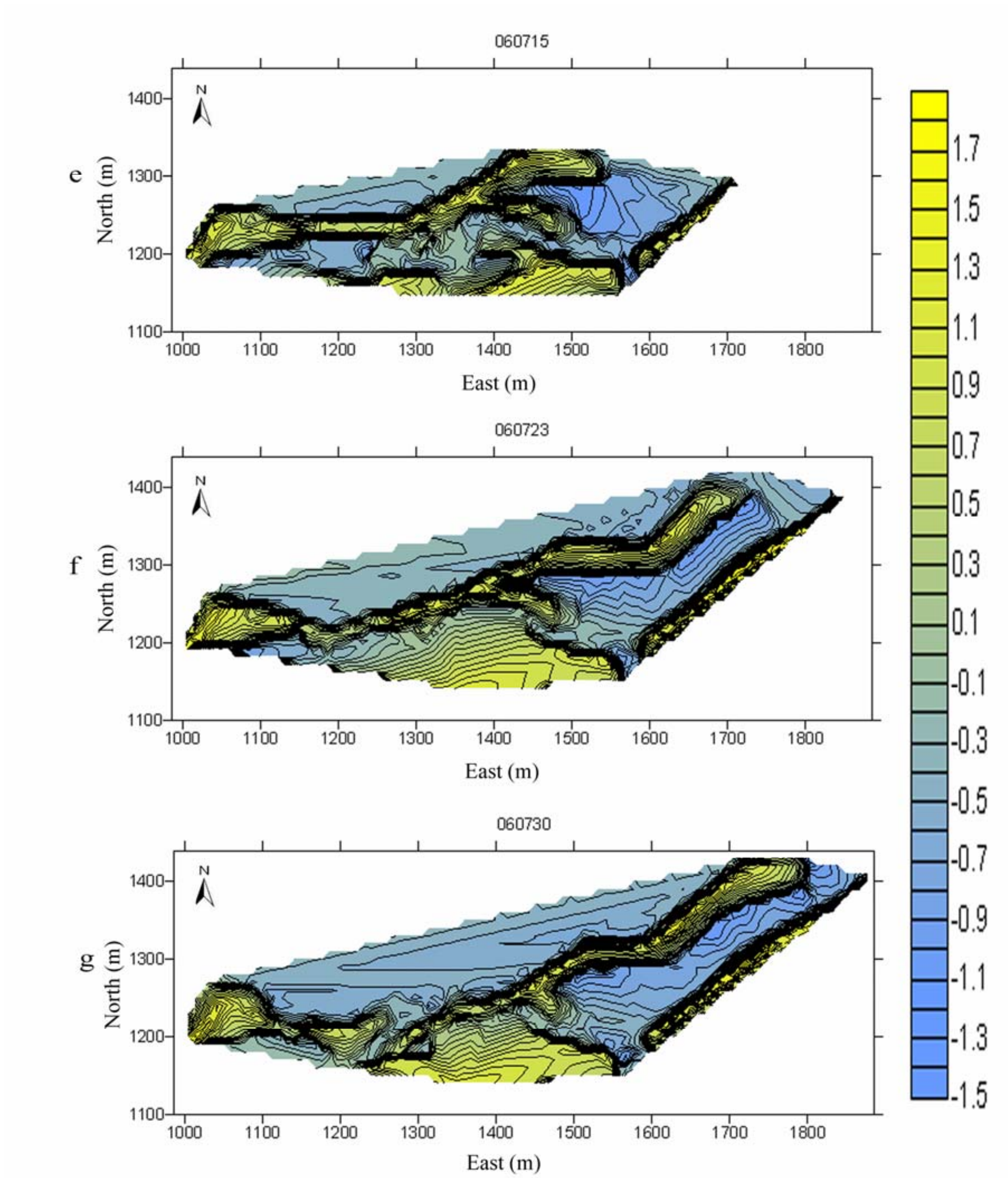

Figure 8: Measured spit and barrier island morphology during the measurement campaign

Figure 8a shows the measured topography on the 28th of May. A sand bar is visible in the plot around 1080-1200 m East and 1270 m North. Probably it has formed when sediment was added to the ebb shoal through continuous sediment bypassing according to FitzGerald (1988), and then by onshore movement the bar has emerged. Between the sandstone reef and the sand bar is a channel located. This channel contributes to the sediment bypassing through its ebb discharge.

Figure 8b shows the study area two weeks later on the 11th of June. The spit growth has now begun due to divergence of the long shore sediment transport through diffraction at the top of the sandstone reef. A similar spit build-up related to longshore sediment transport is presented by Özhan (1987) at the micro-tidal Köycegiz Lake Inlet, Turkey. Between 1150 - 1250 m East and 1250 m North a very thin and low sand bar is located. During high tide it is covered by water since the elevation is only a couple of decimeters above mean sea level. Possibly this is the bar from the 28th of May that has migrated towards the barrier island through onshore movement. The reason for its low elevation could be that waves have eroded the top of the sand bar and moved the sediment into the bay. Between the spit and the sand bar is a channel located which is quite narrow but deep enough to allow small fishing boats to pass.

Figure 8c shows the morphology three weeks later on the 2nd of July. The spit has now grown much longer and it stretches from 1050 - 1300 m East. Part of the spit has migrated landward which is visible between 1150 - 1250 m East. A possible reason might be that this part receives the greatest wave energy which may have caused onshore movement. A pool is located in the middle of the spit that is the result of a second spit emerging from the sea. The second spit has most likely been driven onto the first by onshore movement (Wikramanayake, 060702). To the east of the spit is a banana-shaped sand bar located. This sand bar has emerged from the ebb shoal and moved landward through onshore movement. It is not very clear in Figure 8c, but in the bay the water is now shallower than during the previous weeks since sediment has been carried into the bay. The tide does not seem strong enough to clear the main ebb channel and transport the sediment out to sea again. The inlet has migrated to about 1300 m East and it is shallow. Around 1550 - 1700 m East and 1170 -1200 m North, the waves have eroded the beach on the barrier island that has resulted in a steep beach face which can be seen in Figure 9.

Figure 9: The eroded beach face on the barrier island

Figure 8d shows the inlet almost a week later on the 8th of July. Compared to the previous week the spit is longer and wider. A new sand bar has emerged, around 1300-1450 m East, probably from the ebb shoal. The new bar and the former banana-shaped bar are now connected with the spit. The pool on the spit is still clearly visible and its shape is shown in Figure 10. Almost the entire inlet is closed which causes major problems for the fishermen who needs to push their boats through the shallowest parts (Figure 11).

Figure 10: The pool of water located on the spit

Figure 11: Fishermen pushing their boats in the shallow water between the spit and the barrier island

Figure 8e shows the inlet on the 15th of July. The sand spit is longer and in some areas thinner compared to the earlier week. The pool on the sand spit has decreased in size which indicates that the spit may have migrated landward. At first it might look like material from the spit has moved offshore, but that is not likely because the beach face of the spit (Figure 12), does not have an offshore profile with the characteristic steeply eroded beach face. The inlet is still almost completely closed; therefore a couple of artificial openings was attempted by the local people using a machine, resulting in two unsuccessful attempts on the sand spit and one successful on the barrier island between 1570 - 1600 m East (see Figure 13).

Figure 12: Beach face of the spit

Figure 13: Artificially dug channel for the fishing boats

Figure 8f shows the inlet on the 23rd of July. The sand spit is much longer, compared to the previous week, and it stretches to 1700 m East. A new sand bar has probably emerged and attached to the spit around 1550 m East, and the new bar is oriented in a North-South direction. Again, onshore movement has caused the spit to migrate towards the barrier island which is clearly visible around 1150 - 1300 m East. The migration has given the spit a curved shape, as shown in Figure 14. A reason for the curved shape might be a weakened monsoon which has led to a decrease in the longshore sediment transport implying that no new sediment is added to the spit. During flood this part of the spit is close to the water line which causes the waves to flow over the spit and induce a landward movement. Between the spit and the barrier island quicksand conditions was observed in the shallow water.

The beach erosion, around 1550 - 1700 m East on the barrier island has almost ceased, because the spit provides shelter from the waves. The fishing boat channel that was dug between 8 – 15th of July is wider, which is clearly visible in Figure 8f. Increased water flow through this part takes place when the inlet closes, and the increased flow clears the channel.

Figure 14: Landward migration of the spit

Figure 8g shows the inlet on the 30th of July. The spit is now extending all the way to 1800 m East which results in a total spit growth of about 800 m during the monsoon. Similar observation was made by LHI for the south-west monsoon in 1996 (Lanka Hydraulic Institute, 1998). Again, a new sand bar has attached itself to the very end of the spit and increased in length. The whole spit is thinner and has moved towards the barrier island. A breach of the spit has occurred at 1250 - 1300 m East. The breaching is caused by a mix of a decrease in the longshore sediment transport and a high amount of eroding waves at the specific location. When the new inlet is created it is easier for the water to flow through it instead of through the dug channel in the barrier island. The result over time will be that erosion makes the former inlet wider and deeper, whereas sedimentation fills up the latter one.

Spit Evolution

Properties considering the spit morphology are only presented for the five measurements in July, since the data for the two measurements in May and June do not show a well-defined spit.

The spit length is defined as the unbreached shoreline from the sandstone reef, 1050 m West in Figure 8, to the most eastern point of the sand spit. The variation in the spit length in July can be seen in Figure 15. It is clear that the length increases over time, which corresponds to the results displayed in Figure 8 c-g. The average spit growth rate during July is 13 m/day. The volume change above mean sea level of the spit was calculated in Surfer and the result is presented in Figure 16. According to the plots in Figure 8 the spit grew substantially during the south-west monsoon and the volume calculations here confirm this. The average volume growth rate is calculated to be 360 m^3/day. Finally, the average spit width, shown in Figure 17, was obtained through the cross-sectional area, also calculated in Surfer, and the length. The figure shows that the width varies during July but the maximum difference is only 10 m, with the spit width being 45 m on 060715 compared to 35 m on 060730.

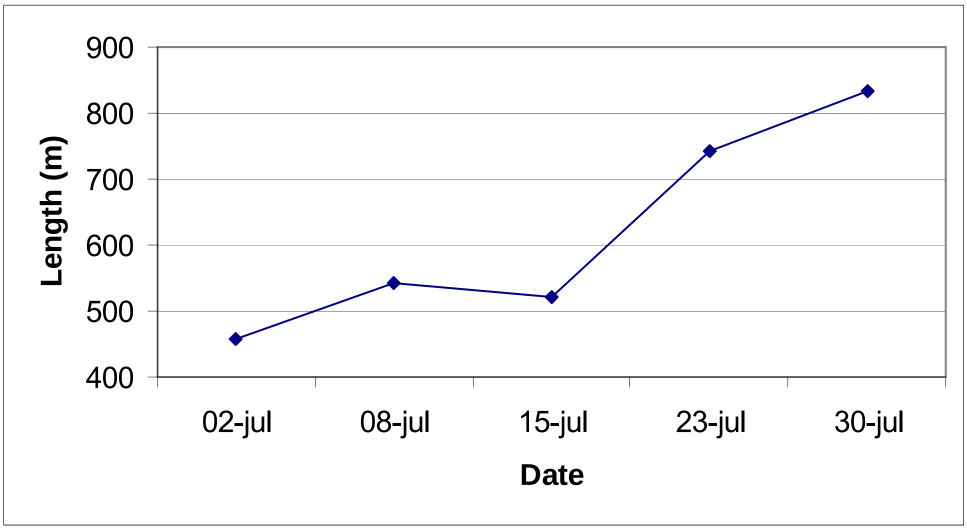

Figure 15: Variation in spit length, 060702-060730

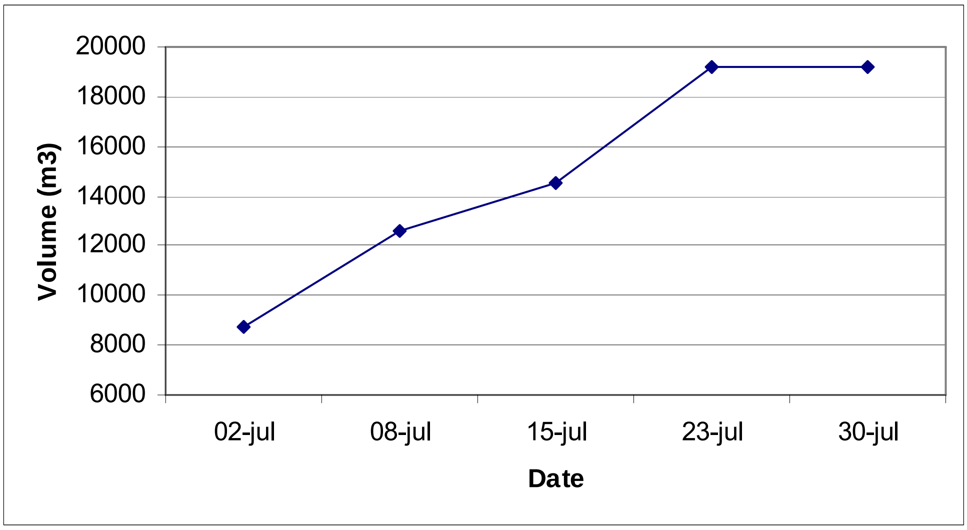

Figure 16: Variation in spit volume above mean sea level, 060702-060730

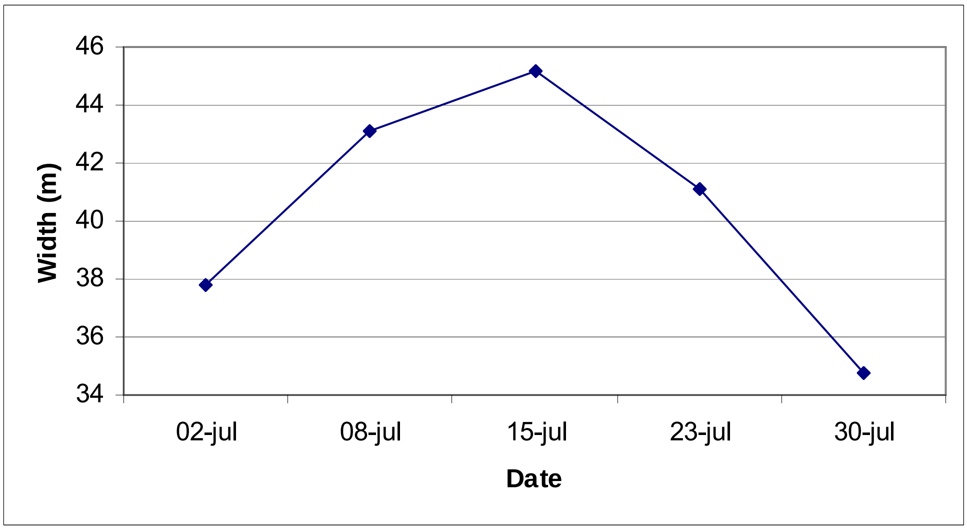

Figure 17: Variation in average spit width, 060702-060730

Inlet Response Modelling

Introduction

The mathematical modelling encompassed two different approaches, namely one basic and one more advanced approach. In the basic model two morphological elements, the reef beach and the spit, is taken to represent the Chilaw inlet and the interaction between those elements are described in a simplified way. The advanced model includes three morphological elements, the two elements in the basic model and the ebb shoal. In the latter model a more detailed description is employed of the interacting processes and sediment pathways at the Chilaw inlet area.

Schematization of Sediment Pathways in the Area

Figure 18 shows the schematized sediment transport pathways and morphological features at Chilaw inlet.

The rate Q_{IN} is the sediment transported into to the area from beaches south of the reef by northerly directed longshore sediment transport. Along the 5.5 km long sandstone reef sediment is added to the longshore sediment transport by erosion of the material deposited on the reef, Q_D. The rates Q_{IN} together with Q_D is the sediment flow to the reef beach volume and will affect the outflow from the reef beach, Q_R.

When the sediment flow, Q_R, reaches the tip of the sandstone reef it is divided into two transport components. One is caused by diffraction behind the tip and results in a sand transport in an easterly direction across the inlet, which initiates the spit growth (Wikramanayake and Pattiaratchi, 1999). The second sediment pathway is to the north-east, and the sediment is here assumed to be transported to an ebb shoal. The ebb shoal connects the sediment pathways from the reef beach, spit, and the down-drift side of the inlet. Sediment comes to the ebb shoal either from longshore transport, Q_R, or from the spit, Q_C, when the inlet current is strong and erodes the tip of the spit. Sediment leaves the ebb shoal through sediment bypassing, Q_{OUT}, or through Q_E which is the wave related cross-shore transport. The amount that bypasses depends on how close the actual volume is to the equilibrium volume, the fuller the reservoir is, the larger the amount that bypasses through Q_{OUT}, according to the reservoir modeling concept introduced by Kraus (2002). The rate Q_E may be transported in two different directions: waves lower than a threshold wave height taken to be 0.45 m results in a sediment transport from the ebb shoal to the spit through onshore movement. For opposite conditions, wave height higher than 0.45 m, the waves will erode the ebb shoal and sediment will be lost to the sea. See *Appendix 4 – Sediment Loss from Ebb Shoal*.

In the more advanced model, spit growth is governed by diffraction but also by onshore movement from the ebb shoal, Q_E. The spit loses sand by erosion caused through the inlet flow, towards the bay and the ebb shoal. The inlet flow is crucial early in the monsoon when the channel flow is strong since the spit has not yet deflected the channel. In the mid-to-late monsoon when the spit has grown larger the water is forced to take another way and therefore only affects the spit growth to a limited degree.

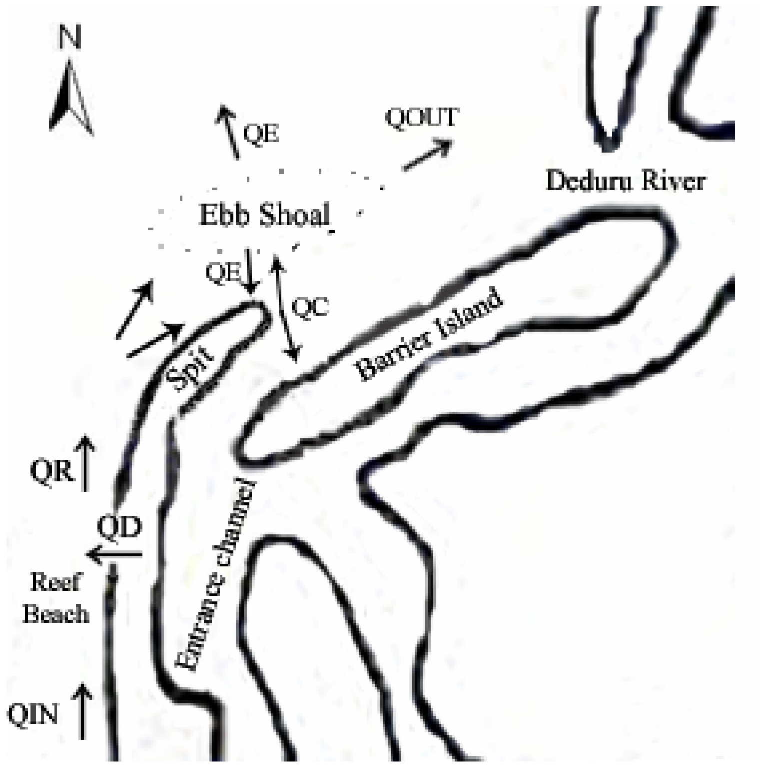

Figure 18: Schematized sediment pathways and morphological features at Chilaw inlet

Basic Model

Introduction

In the basic model two of the morphological elements are included, namely the reef beach and the sand spit, and these are represented as boxes in Figure 19. Each morphological element is characterized by its volume and the sediment transport relationships are dependent on this volume as well as external variables such as the wave properties. Figure 19 shows the schematization of the sediment pathways, where Q_{IN} represents the north-going longshore transport, Q_D is the sediment transported from the dune exposed to erosion from wave runup and Q_R is the outflow from the reef beach. The volume at a certain time and the equilibrium volume in the reef beach are V_R and V_{RE}, respectively, whereas W_S is the constant sand spit width and D_S the vertical extension depth, i.e., the depth of closure for the spit. A coefficient δ is used to determine the proportion of sediment from Q_R that enters the sand spit, and this coefficient will affect the spit volume, V_S, and spit length, L_S. According to Kraus (1999) a spit can grow under different conditions. In the Chilaw basic modelling case an unrestricted spit growth is assumed, which means that no sediments will leave the spit.

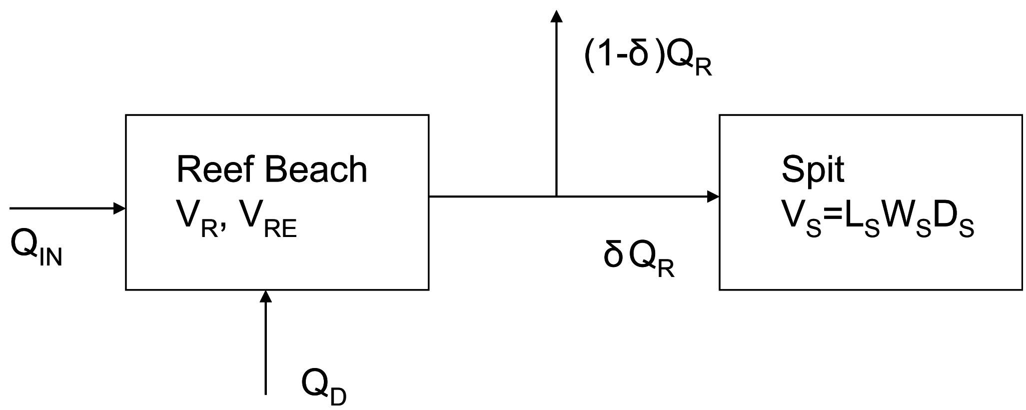

Figure 19: Schematization of basic model for spit growth

Input Data and Assumptions

For the Chilaw area wave measurements were undertaken from November 1995 to May 1997 with some gaps in between (Wikramanayake, 2003). Although the wave measurement campaign was performed 1995-1997, the data from it will be used in this study as representative since the wind conditions follow a certain pattern during the monsoon (Wikramanayake, 2006-07). For a period of 3 weeks in late May wave data concerning direction is missing and had to be estimated based on data from early May and August. Complete wave data is also missing for the last 2.5 weeks in July and had to be estimated based on the overall wave data, that is, direction, height, and period before and after the gap. The wave direction, height, and period, varies over time.

A potential north-going longshore sediment transport was estimated for each day during the period 1st of May to 31st of August. The estimation was based on the daily average wave direction, and the daily average significant wave height and period for data obtained from May to August 1996 (Wikramanayake, 2006). All data concerning waves include both sea and swell waves. The potential longshore sediment transport assumptions, basic equations, and results are presented in *Appendix 1 - Long shore Sediment Transport*.

The amount of sand transported from the dune is estimated from interpretations of the shore profiles in Lankan Hydraulic Institute report (1998). Profile surveys of the dune region before and after the summer monsoon gave a basis for estimating the average eroded volume per unit time for this region. A representative average sand flow of 650 m^3/day was used in the model.

The equilibrium and start (initial) volume in the reef beach were estimated to 70 000 m^3 and 10 000 m^3, respectively, in the basic model. As seen in the morphology plots (Figure 8) the spit growth is limited the first month of the monsoon and later on the spit length increases. The sediment output from the reef beach depends on the ratio between the actual volume and the equilibrium volume in the reef beach. A small sediment output results in a limited spit growth, which is the case early in the season when the start volume is small compared to the equilibrium volume. When using the values of 70 000 m^3 and 10 000 m^3 for equilibrium and start volume, respectively, the model behaves similarly to the observed spit growth in Figure 8.

The coefficient δ is an important quantity in the basic model, since it determines how much of the longshore sediment transport that will be transported to the spit. When using a $\delta = 0.55$ a spit length of approximately 800 m in late July is obtained, which corresponds well to the observations in Figure 15. According to Wikramanayake and Pattiaratchi (1999) more sediment is added to the spit than bypassed across the inlet. A δ value of 0.55 might therefore be appropriate.

An average spit width of 40 m was calculated based on the information from Figure 17, and this value was used in the basic model.

The spit is assumed to grow with a constant active depth, known as the depth of closure. This is defined as the seaward depth of which repeated field measurements over long-time scales does not find any changes of the seafloor elevation (US Army Corps of Engineering, 2006). According to the Coastal Engineering manual (2006), the depth of closure can be calculated by using the effective significant wave height. Applying data from Wikramanayake (2006) for the summer monsoon period a depth of closure corresponding to 4.5 m is obtained for Chilaw inlet. For further information on the calculations, see *Appendix 2 – Depth of Closure.*

General Equations

The change in sediment volume over time for the two morphological elements in the basic model, shown in Figure 19, are governed by sand conservation equations, which may be written as:

$$\frac{dV_R}{dt} = Q_{IN} + Q_D - Q_R \qquad (1)$$

$$\frac{dV_S}{dt} = \delta Q_R \qquad (2)$$

where V_R is the sediment volume stored along the reef beach, t time, Q_{IN} the sediment flux into the reef beach from the areas further south, Q_D the sediment flux to the reef beach from the subaerial portion of the beach (erosion of the reef dune), Q_R the outflow of sediment from the reef beach, δ a coefficient determining how much of Q_R that is transported to the spit, and V_S the volume of sediment stored in the spit.

The outflow of sediment from the reef beach is modeled using the reservoir concept introduced by Kraus (2002):

$$Q_R = \left(Q_{IN} + Q_D\right)\frac{V_R}{V_{RE}} \qquad (3)$$

where V_{RE} is an equilibrium volume characterizing the amount of sediment that may be stored in the area seaward of the reef. Combining the Equations 1 and 3 yields:

$$\frac{dV_R}{dt} = \left(Q_{IN} + Q_D\right)\left(1 - \frac{V_R}{V_{RE}}\right) \tag{4}$$

For unrestricted spit growth, Kraus (1999) gives the equation:

$$\frac{dL_S}{dt} = \frac{\delta Q_R}{W_S D_S} \tag{5}$$

where L_S is the spit length, W_S the spit width, and D_S the vertical extension of the spit or depth of closure, V_S=$L_S W_S D_S$. Both W_S and D_S are set to be constant in the present model.

Solution Method

Equation 3, 4, and 5 were discretized and a time step of Δt = 1 day was used when solving the equation system in MATLAB:

$$V_R^{i+1} = V_R^i + \Delta t\left(Q_{IN}^i + Q_D\right)\left(1 - \frac{V_R^i}{V_{RE}}\right) \tag{6}$$

$$Q_R^i = \left(Q_{IN}^i + Q_D\right)\frac{V_R^i}{V_{RE}} \tag{7}$$

$$L_S^{i+1} = L_S^i + \Delta t \frac{\delta Q_R^i}{W_S D_S} \tag{8}$$

where *i* is an index. For *i*=1 the initial values on the volume in the reef beach is employed and Q_{IN}^i is calculated from the longshore sediment transport formula based on the input wave data. In total the simulation period included 123 time steps, corresponding to the days in May, June, July and August. The calculations resulted in a time series of 123 different spit lengths for the studied period.

Basic Model Result and Discussion

The resulting spit growth for the basic model and the measured spit length in July is presented in Figure 20. After 90 days, approximately the 30th of July, a spit length of about 800 meters is obtained in the model. This value corresponds well to the results of the measured spit length in July 2006. The actual spit length increased about 370 m in July 2006 while the basic model shows an increase of about 260 m. From observations and morphological plots (Figure 8) it seems like the spit grows slowly early in the monsoon, during May and June, and later, in July, the growth is accelerated. The basic model shows this behavior; the first 50 days the spit growth is retarded and after that the spit seems to grow at almost constant speed. The constant speed is obtained when the reef beach has reached its equilibrium volume and all the sediment input is bypassed. A larger reef beach equilibrium volume as well as a lower δ value will result in a shorter spit length.

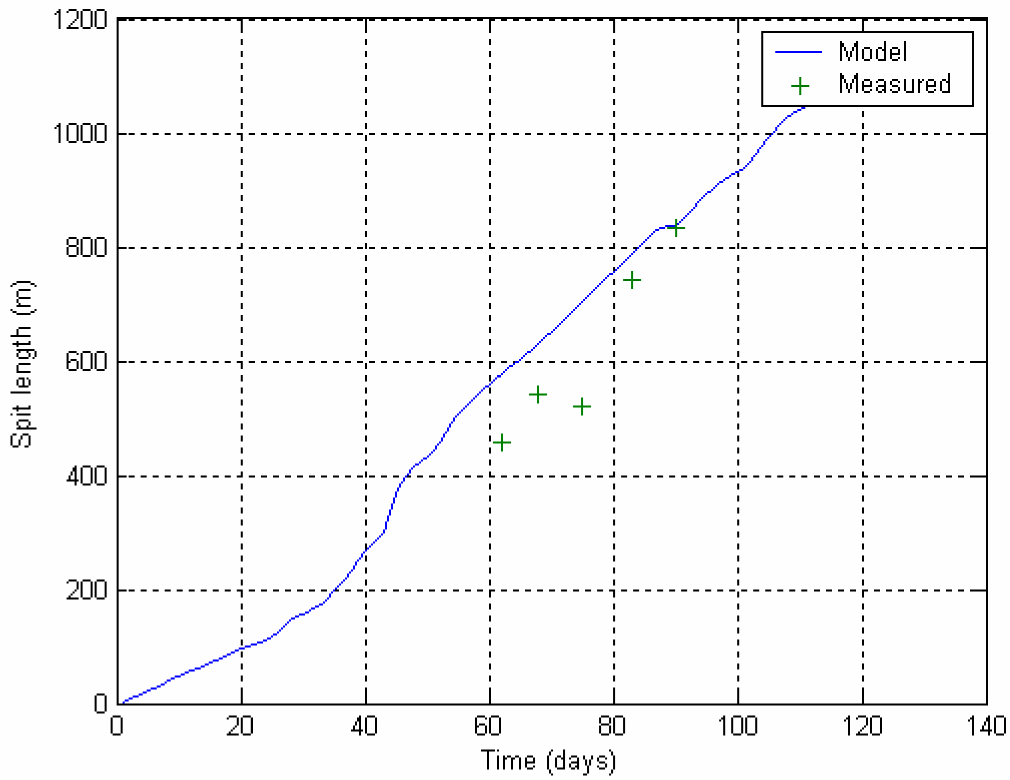

Figure 20: Spit growth during the south-west monsoon, based on δ = 0.55 (The spit growth start in May and ends in August)

Sensitivity Analysis of Basic Model

The most important parameter in the basic model is δ, which in some sense quantifies the influence of diffraction around the edge of the reef. Figure 21 shows the spit growth for different values on δ, where a higher value gives a longer spit for the studied period. A δ value of 0.55 was chosen since it represents a spit length of approximately 800 m after 90 days, which corresponds to the observed length presented in Figure 15.

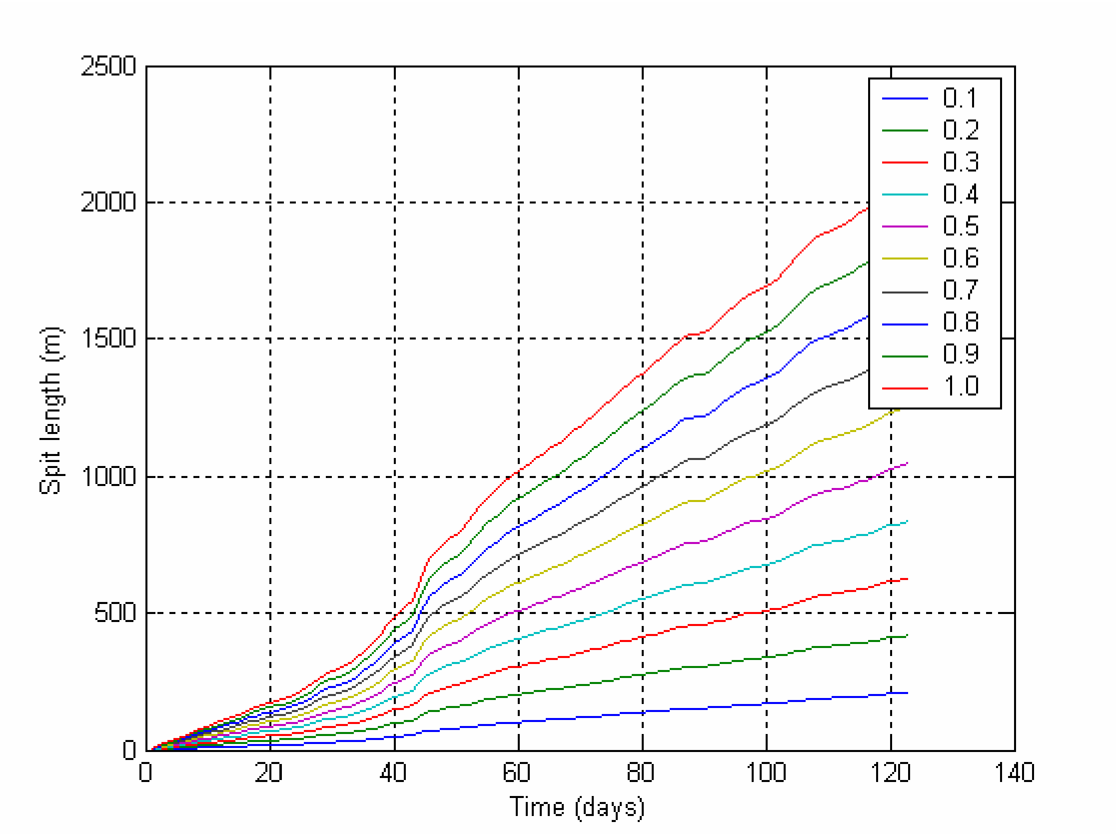

Figure 21: Spit growth for different values on δ in the interval 0.1 - 1.0

Figure 22 illustrates the spit growth for varying equilibrium volumes of the reef beach. It is clear that the size of the equilibrium volume affects the spit growth less compared to the influence of δ. Even if the equilibrium volume is large, 110 000 m^3, and there is a gradual outflow from the reef beach, the north-going longshore sediment transport fills the reef beach quite fast, and then all sediment is bypassed. The reason for this is the relatively large longshore sediment transport rate, in average 2800 m^3/day, and the sediment from the dune, 653 m^3/day.

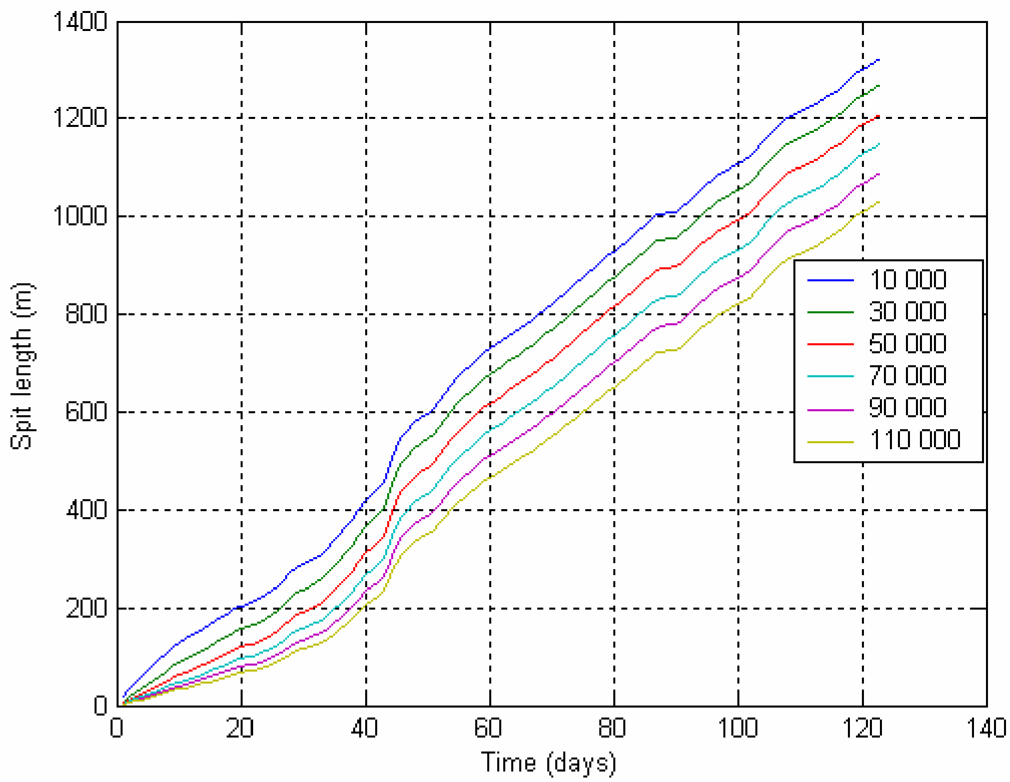

Figure 22: Spit growth for different equilibrium volumes for the reef beach in the interval 10 000 - 110 000 m^3

Advanced Model

Introduction

The advanced model includes three morphological elements: the reef beach, the ebb shoal, and the spit. Figure 23 illustrates the morphological elements and sediment pathways. The sediment transport along the sandstone reef is described by the reef beach box, and sediment is added from longshore sediment transport, Q_{IN}, and from the dune, Q_D. A more sophisticated description of the transport Q_D from the dune compared to the basic model is employed, where runup height exceeding the reef elevation determines the eroded volume. The reef beach has an equilibrium and start volume denoted as V_R and V_{RE}, respectively, in Figure 23. The sediment outflow from the reef beach, Q_R, is split in two components; one to the ebb shoal and one to the spit. As before, δ is a coefficient quantifying the influence of diffraction that determines the size of the flow in each component.

The ebb shoal has an equilibrium and start volume, V_{EE} and V_E, respectively. The rate Q_E represents a cross-shore sediment transport term, and if the significant wave height is less than 0.45 m sand transport is towards the spit, whereas for a height greater than 0.45 m it is towards the ocean. Sediment is also bypassed out of the system, via the ebb shoal, and transported further north along the coast, Q_{OUT}.

The spit is assumed to grow with a constant width and depth, W_S and D_S. Sediment is added to the spit by $\delta\, Q_R$ and Q_E and lost through Q_C, which is the sediment eroded from the spit by the inlet channel flow. The empirical coefficient ε determines the portion of Q_C that is transported to the ebb shoal and $(1-\varepsilon)Q_C$ is the amount deposited in the bay.

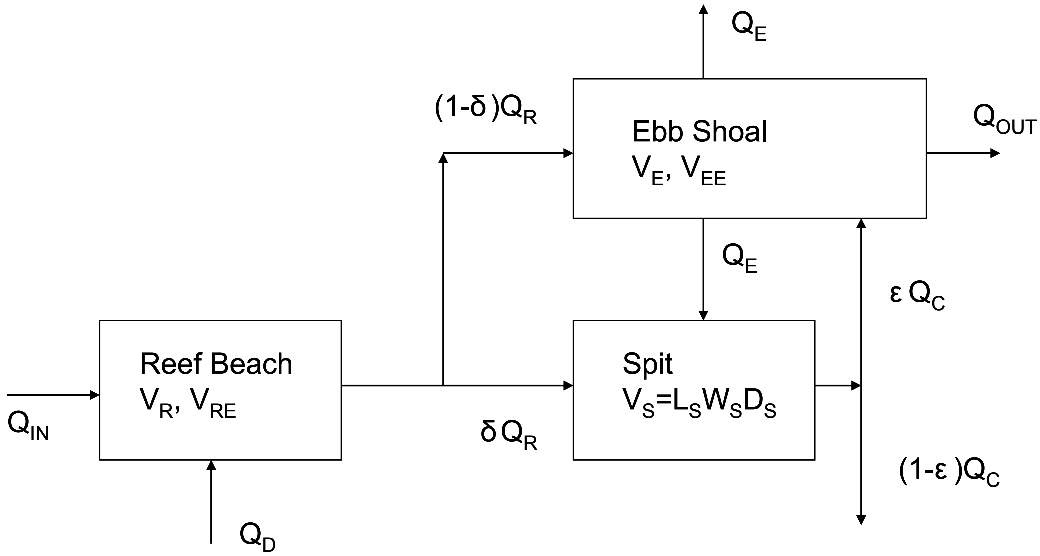

Figure 23: Schematization of advanced model

Input Data and Assumptions

To the reef beach box enters the longshore sediment transport, Q_{IN}, and the sediment from the dune, Q_D. The same data and assumptions concerning Q_{IN} as for the basic model are applicable here. However, the input sediment from the dune on the sandstone reef is estimated from the impact model for dune erosion (Larson et al., 2004). This model is based on the runup height and the reef elevation above mean sea level, see *Appendix 3 - Sediment Transport from Reef Dune*. The start and equilibrium volume for the reef beach used in the advanced model is 10 000 m^3 and 70 000 m^3, respectively. These values are to be regarded as approximations with the same assumptions valid as for the basic model.

The dimensionless coefficient δ is also used in the advanced model. A δ-value of 0.55 determined from the basic model simulations is used based on the discussion presented above.

Continuous bypassing along the ebb shoal transports sand past Chilaw inlet and further north along the coast. Similar to the reef beach the bypassing at the ebb shoal is proportional to the ratio V_E/V_{EE}. The ebb shoal equilibrium volume was estimated according to the formula presented by Walton and Adams (1976). When trying to estimate the volume of sand stored in an ebb shoal, either the tidal prism or inlet channel cross section could be used to predict this volume (Walton and Adams, 1976). At Chilaw inlet a tidal prism at the entrance channel of 2.45 Mm^3 was employed (Wikramanayake and Pattiaratchi, 1999). Three classifications based on the wave height, H, and wave period, T, are presented in Walton and Adams (1976): mildly, moderately, and highly exposed coastlines. When using the average significant wave height and period at Chilaw from Wikramanayake (2006) a classification value of about 600 is obtained, and this corresponds to a highly exposed coastline. By use of the tidal prism and the previous classification, a sand volume in the ebb shoal is estimated according to the formula given by Walton and Adams (1976). The result is an ebb shoal volume of 6 300 m^3 sand. This result is probably an underestimation of the volume because the ebb shoal is located in the much calmer water that forms behind the sandstone reef. Volume calculations are therefore also performed for both moderately and mildly exposed coastlines, with the same tidal prism of 2.45 Mm^3. An average volume for the three classifications is 8 000 m^3, and this value is used in the advanced model. The ebb shoal is assumed to contain about 4 000 m^3 sand when the south-west monsoon starts. These deposits derive from high discharge, carrying sediment, in Deduru river during the inter-monsoon rains in October and November (Wikramanayake and Pattiaratchi, 1999).

The exchange of sediment between the ebb shoal and the spit, Q_E, is difficult to quantify through simple relationships. Qualitatively, sediment moves offshore in the cross-shore direction when $H_{SO}/wT > 3$, where w is the sediment fall speed, and onshore when $H_{SO}/wT < 3$ (Kraus et al., 1991). Thus, assuming no change in the sediment properties and a wave period that is more or less constant, sand will be supplied from the shoal to the spit if the wave height is less than 0.45 m. In this calculation a fall speed of 0.025 m/s, a median grain size of 0.2 mm, a temperature of 20ºC, and a wave period of T=6 sec was assumed. For additional information on how to calculate Q_E see *Appendix 4 – Sediment Loss from Ebb Shoal* (Kraus and Larson, 2001).

In the advanced model, the ebb shoal will lose sediment both through onshore and offshore transport. The spit will receive sediment from the ebb shoal when onshore movement occurs, and the ebb shoal loses material to deeper water when offshore transport conditions occur. In the present model the spit does not supply the shoal with material during erosive conditions. Such a sediment pathway is easy to include in the model, but implies a more complex system with stronger coupling between the spit and the shoal.

An average spit width of 40 m was calculated based on the information from Figure 17, and this value was used in the advanced model as well. The spit is assumed to grow with a constant depth of closure, as in the basic model, and a value of 4.45 m was used. The same assumptions and equations are used as in *Appendix 2 – Depth of Closure*.

The transport rate Q_C can be obtained from the water velocity in the channel. According to Wikramanayake and Pattiaratchi (1999) the maximum ebb discharge in the channel is 178 m^3/s and from the relationships proposed by Walton and Adams (1976) the cross-sectional area at the throat can be calculated, if the ebb shoal volume is known. Depending on the classification of the inlet, mildly, moderately, or highly exposed, three different values on the cross-sectional area can be obtained. Since it is difficult to decide whether Chilaw is highly or mildly exposed, an average value on the velocity was used, 1.9 m/s. From this velocity Q_C = 200 m^3/day is obtained, see *Appendix 5 - Sediment Eroding from Spit*.

The non-dimensional parameter ε is an empirical coefficient that determines the portion of Q_C that is transported to the ebb shoal and to the bay. A value of ε=0.5 was used in the model since the ebb and flood flow are assumed to be about the same.

General Equations

The evolution of the morphological elements, that is the reef beach, ebb shoal, and spit, is governed by three sand conservation equations according to:

$$\frac{dV_R}{dt} = Q_{IN} + Q_D - Q_R \quad (9)$$

$$\frac{dV_E}{dt} = (1-\delta)Q_R + \varepsilon Q_C - Q_E - Q_{OUT} \quad (10)$$

$$\frac{dV_S}{dt} = \delta Q_R + Q_E - Q_C \quad (11)$$

where V_E is the volume in the ebb shoal, Q_E the sediment loss from the ebb shoal, Q_C the sediment eroded from the spit, and ε determines the amount of sediment that is deposited in the bay and on the ebb shoal.

The output of sediment from the reef beach, Q_R, and the ebb shoal, Q_{OUT}, is modeled using the reservoir concept (Kraus, 2002), where the transport from a morphological element is proportional to the input of sediment and the degree to which the maximum (equilibrium) volume of the element is filled up:

$$Q_R = \left(Q_{IN} + Q_D\right)\frac{V_R}{V_{RE}} \tag{12}$$

$$Q_{OUT} = \left(\left(1-\delta\right)Q_R + \varepsilon Q_C\right)\frac{V_E}{V_{EE}} \tag{13}$$

where V_{EE} is the equilibrium volume of the ebb shoal.

An inflow of sand corresponding to $Q_S=\delta Q_R+Q_E$ occurs to the spit and if this feature maintains an equilibrium cross section, deposition of sand will cause an increase in the spit length. Depending on the relationship between Q_S and Q_C, different scenarios regarding the spit evolution and the inlet cross-section are possible:

1. $Q_S > Q_C$ spit growth with reduction of inlet cross section and/or inlet migration
2. $Q_S = Q_C$ equilibrium with no spit growth and stable inlet cross section
3. $Q_S < Q_C$ increase of inlet cross section and decrease in spit length

It will be assumed that case 1 is prevailing for Chilaw inlet during the south-west monsoon. A first approach is to let the spit grow unrestricted, with a constant Q_C, at the same time as the channel migrates East at identical speed. This implies that the channel maintains the transport capacity Q_C and that the excess transport Q_S-Q_C will produce the spit growth.

The growth of the spit may be computed from:

$$\frac{dL_S}{dt} = \frac{Q_S - Q_C}{W_S D_S} \tag{14}$$

where Equation 11 was used assuming $V_S=L_S W_S D_S$ (W_S and D_S being constants because of equilibrium conditions for the spit in the cross-shore direction).

Solution Method

Equation 3, 4, 14, and 30 were discretized. Furthermore, Q_{OUT} in Equation 10 was replaced by Equation 13 and the resulting equation was also discretized. A time step of one day was used, as before, when solving the equation system in MATLAB. The model solves the equations starting with the reef beach box, proceeding with the ebb shoal, and finally solves for the spit box (this solution method results in a one step time delay for the flows and volumes in the whole system, since values from the previous loop are used):

$$V_R^{i+1} = V_R^i + \Delta t \left(Q_{IN}^i + Q_D^i \right) \left(1 - \frac{V_R^i}{V_{RE}} \right) \tag{15}$$

$$Q_R^i = \left(Q_{IN}^i + Q_D^i \right) \frac{V_R^i}{V_{RE}} \tag{16}$$

$$Q_E^i = \frac{\xi_i}{\xi_{cr}} \left(1 - \frac{\xi_i}{\xi_{cr}} \right) \frac{V_E^i}{T_E} \tag{17}$$

$$V_E^{i+1} = V_E^i + \Delta t \left(\left((1-\delta) Q_R^i + \varepsilon Q_C^i \right) \left(1 - \frac{V_E^i}{V_{EE}} \right) - \left| Q_E^i \right| \right) \tag{18}$$

$$Q_S^i = \delta Q_R^i + Q_E^i \tag{19}$$

$$L_S^{i+1} = L_S^i + \Delta t \frac{Q_S^i - Q_C^i}{W_S D_S} \tag{20}$$

When solving the system of equations, a simulation period of 123 time steps, corresponding to the days in May, June, July and August, was employed. Before simulations started, initial values for V_R and V_E had to be set, as previously discussed. Based on the wave characteristics, Q_{IN}, Q_D, and Q_E was calculated every time step using the procedures and equations presented above.

Advanced Model Result and Discussion

Figure 24 shows the modeled spit growth during the south-west monsoon using the advanced model. After 90 days the spit has reached a length of about 800 m which is close to the observed spit growth of fully 800 m. In the advanced model more parameters are included than in the basic model. More parameters requires more data for validation and may result in greater uncertainty, and if they are improperly calculated or even just estimated based on limited data they can bring errors into the model. Despite the increased numbers of parameters the resulting spit growth in Figure 24 is closed to the observed.

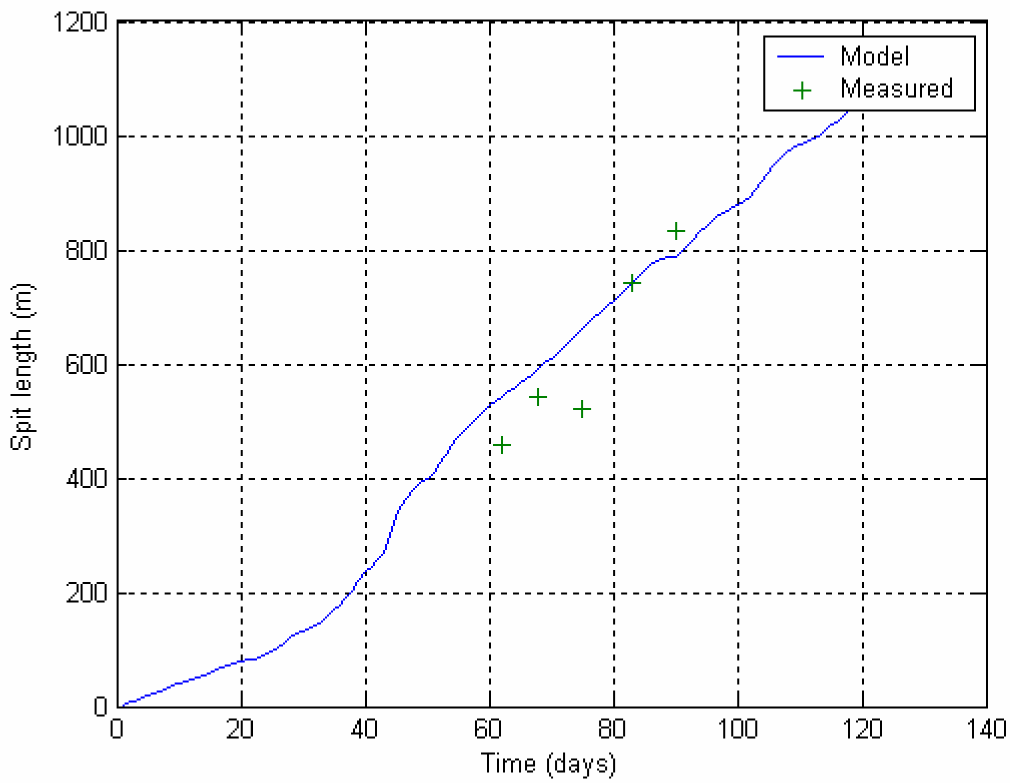

Figure 24: Spit growth during the south-west monsoon, (based on δ = 0.55 and ε=0.5; the spit growth starts in May and ends in August)

Sensitivity Analysis of Advanced Model

Figure 25 shows the spit growth for various values on Q_C. It is clear that a high value on Q_C will result in a decreased spit growth since sediment is removed (eroded) from the spit. For very high Q_C the spit can not grow at all since all the sediment added is immediately removed by the channel flow. The first 50 days a large part of the long shore sediment transport is added to the reef beach box and therefore small amounts of sediment is bypassed to the spit. During this period Q_C has a large impact on the spit growth. After 50 days the reef beach sediment volume has increased and the sediment outflow is hence larger. The influence of Q_C is smaller during this period. Depending on Q_C and Q_S the resulting spit length after 120 days can differ a lot. Since Q_C has a great influence on the spit growth, especially in May and June, it is important to have accurate input values on the variables that are used to determine Q_C.

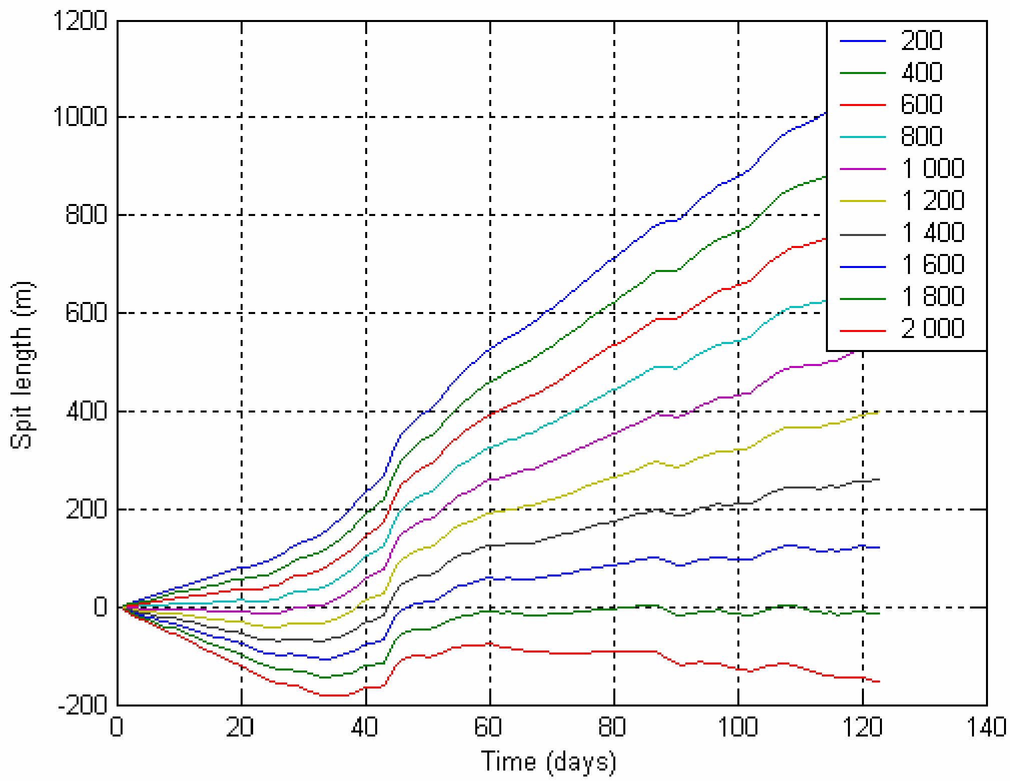

Figure 25: Spit growth for different values on Q_C in the interval 200 – 2 000 m^3/day

The coefficient κ, which quantifies the influence of diffraction on the wave height used to determine Q_E, affects the size and direction of Q_E, Figure 26 illustrates the behavior of Q_E for different values on κ. A positive value on Q_E results in an onshore transport from the ebb shoal to the spit and a negative value yields an offshore transport. The critical values are $\kappa > 0.3$, for which Q_E changes to be only negative. If $\kappa > 0.4$, the result is an unrealistic amount of offshore transport. It was seen that onshore movement was the dominant process since large sand packages moved onshore towards the spit during the measurement campaign, see chapter Overview of Morphological Change. From time to time the waves were large, indicating a possible offshore transport. A κ value of 0.3 results in both onshore and offshore movement, which corresponds to the observed processes at Chilaw inlet and was therefore used in the modelling.

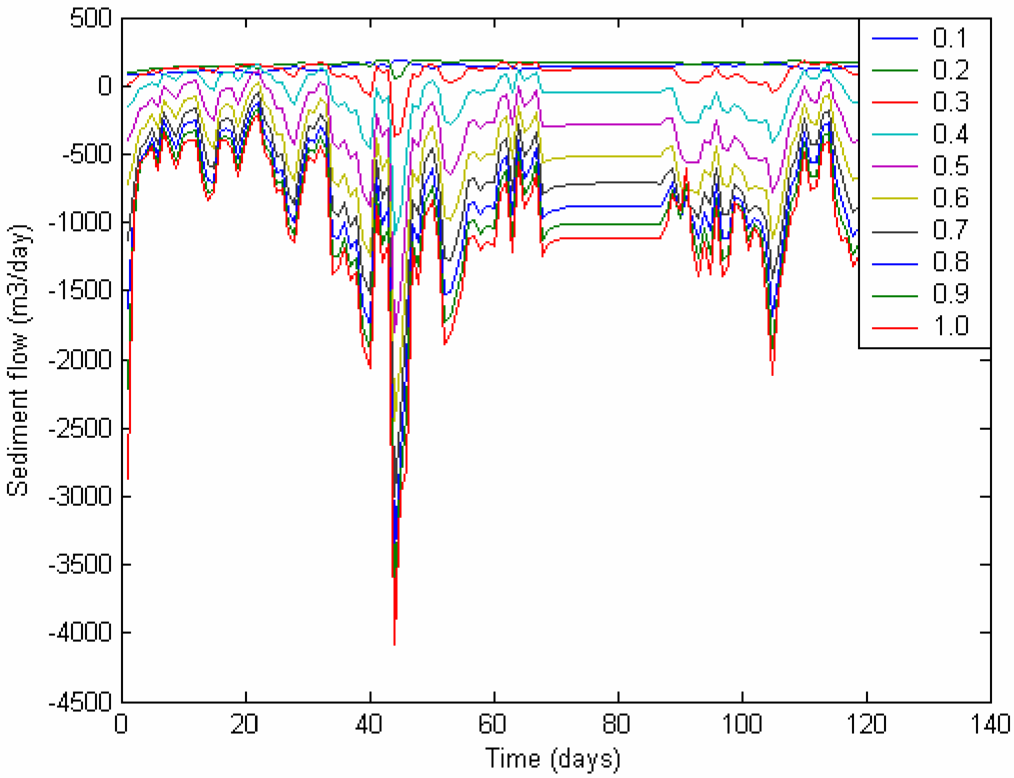

Figure 26: Transport from the ebb shoal (Q_E) as a function of time for different values on κ in the interval 0.1 - 1.0

Since Q_E defines sediment loss from the ebb shoal, the shoal volume will also be greatly affected by high values on κ. This is clearly displayed in Figure 27 where the ebb shoal volume is plotted for different values on κ. The equilibrium volume for the shoal is 8000 m^3 and for small κ -values the volume almost reaches this value after 40-50 days. However, for κ close to one the shoal is reduced to about 25 percent of its equilibrium volume. In the beginning of the period large amounts of sediment is trapped in the reef beach box and therefore only a small amount is bypassed to the spit and ebb shoal. Since the monsoon continues throughout the simulation period and the sediment transport is abundant, the ebb shoal volume should be close to its equilibrium volume. When considering the ebb shoal volume a κ -value of 0.3 seems reasonable.

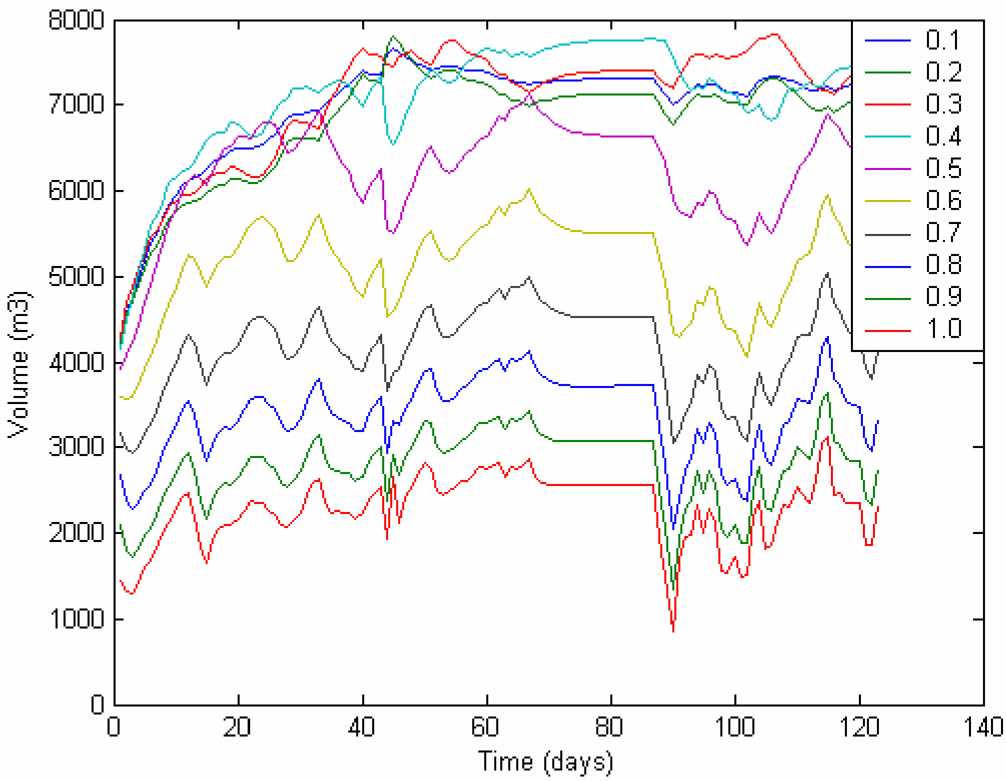

Figure 27: Ebb shoal volumes as a function of time for different values on κ in the interval 0.1 - 1.0

Comparing Basic and Advanced Model

Both the basic and the advanced model include many simplifications in the description of the morphological elements, sediment pathways, and interacting processes present at Chilaw inlet. The basic model consists of only two boxes but the resulting spit length is, despite this, close to the observed spit growth presented in Figure 15. One reason for this is that the parameters included in the model, such as the longshore sediment transport rate and the sediment supply from the reef dune, and the spit characteristics, width and depth of closure, were calculated based on measured input data. Only equilibrium and initial volumes related to the reef beach together with δ were estimated. In the sensitivity analysis changes in the reef beach equilibrium volume had limited influence on the model behavior. The coefficient δ affected the model behavior significantly and was therefore tested in the sensitivity analysis in order to establish a suitable value.

In the advanced model more parameters are included. The dimensionless coefficient ε, as well as the variables Q_E and Q_C, were new parameters for this model. Even though the values of Q_E and Q_C were based on data, such as wave climate and tidal prism, they involve considerable uncertainties, including the value of κ, which is another dimensionless coefficient that had to be estimated. The resulting plot of the spit length, Figure 24, for the advanced model shows that the model describes the measured spit growth fairly well, compared with Figure 15.

When comparing the results from the basic and advanced model (see Figure 20 and Figure 24, respectively), it is obvious that both provide fairly good representations of the observed spit growth at Chilaw inlet. The advanced model does not produce significantly better results, even though it represents a more detailed description of Chilaw inlet spit growth. Thus, the basic model might be the preferable one with respect to the limited data available for the modeling. In the case of more data available for testing the various components in the advanced model, it is expected that better simulation results would be achieved since the model resolves more of the processes shaping the inlet than the basic model.

Improvements of Model

First, to be able to obtain more accurate results, a complete wave data set for the south-west monsoon 2006 is needed (or for the particular time period to be simulation). When analyzing wave data and morphological maps from the same year, correlations between extreme wave events and morphological spit changes could be done.

Not all sediment pathways are included in the models. In reality a sand transport from the spit to the barrier island caused by onshore movement occurs. It is however very hard to estimate the amount of material that attach to the barrier island each week, since it is difficult to distinguish/define the two morphological elements; spit and barrier island. To be able to measure the morphology of the barrier island more resources, in particular time and labor, are needed. Further, sand is transported offshore from both the spit and barrier island, which is not considered in any of the models. An offshore transport might have a slightly negative effect on the spit growth but some of the sand on the barrier island would be transported to the ebb shoal and then perhaps back to the spit which would increase the spit growth again. If sufficient data for these sediment movements and morphological changes existed a more detailed model could be described.

A more complex model would take into account the reduction in the channel width, with an associated decrease in sediment eroded from the spit, Q_C. In such a model Q_C might eventually become zero, corresponding to inlet closure. Channel migration should still be included, which may further complicate things. The task remains for this scenario, however, to estimate the ratio between channel infilling, which reduces the inlet width, and channel migration, which may occur under maintained transporting capacity.

Conclusions

This study focused on three objectives: to gain increased knowledge about tidal inlets and closure mechanisms and apply this theory to understand the processes around Chilaw inlet; to create topographic maps from measurement data obtained during the south-west monsoon; and to develop a mathematical model which describes the spit growth at Chilaw inlet.

Mechanisms for Inlet Closure

Three major morphological events were observed during the measurement campaign at Chilaw inlet: spit formation, inlet closure, and spit breaching. The spit growth is initialized when the south-west monsoon and thus the northerly directed longshore sediment transport starts. It is a combination of longshore and onshore sediment transport that causes the spit growth. When the longshore current, which carries the sediment along the beach, is interrupted by the Chilaw inlet, the sediment is carried east, around tip of the sandstone reef, and initiates the spit growth. As long as the monsoon continues the spit increases its length and eventually the inlet will close. During the summer of 2006 the inlet closure occurred around the 8-15th of July. The longshore sediment transport does not only affect the spit but, sediment is also transported to the ebb shoal located seaward of the spit. Sediment from the ebb shoal is transported onshore during certain wave conditions and is attached to the spit due to wave refraction and diffraction. Later in the monsoon, the 30th of July, a spit breaching is observed. The breaching is caused by a combination of decreased longshore sediment transport and a large amount of wave energy at the spit. Important to notice is that the growth and breaching of the Chilaw spit not only is a result of one process, but interaction between longshore sediment transport and cross-shore movement is typically the cause. The amount of cross-shore movement is hard to quantify but the longshore sediment transport seems to be the most important process regarding Chilaw inlet closure.

Overview of Morphological Changes

Four morphological elements were identified at Chilaw inlet: the reef beach, the spit, the ebb shoal, and the barrier island. The topographic maps show that a spit growth takes place during the south-west monsoon and especially high growth rate is observed in late July. The spit is getting longer during the measurement campaign and at some locations it moves onshore, towards the barrier island. The water in between the spit and barrier island seems to become gradually shallower due to onshore movement of sediment from both the spit and the ebb shoal. The spit growth causes an inlet closure which restricts the access to the sea for the fishermen, who by mid-July dig a canal in the barrier island. By the end of July a natural spit breaching occur. It is difficult to make a comprehensive analysis of the morphological evolution in the area based on the maps since no measurements were undertaken in the bay or on the slopes of the spit below a water depth of approximately 1 m. However, the maps represent a fairly good representation of the major morphological changes present in the area during the south-west monsoon 2006.

Mathematical Model

Two mathematical models describing Chilaw inlet spit growth were developed and applied, one basic model and one more advanced model. In both cases the modeled spit growth corresponds reasonably well to the measured spit length obtained from the measurement campaign of 2006. The advanced model is based on a more detailed description of the interacting processes and morphological elements and thus includes a couple of more assumptions than the basic model. With regard to the amount of existing data, the preferable model to use is the basic one since it requires less data for validating coefficient values in the model. The most important parameters when modelling Chilaw inlet is the amount of longshore sediment transport and the coefficient δ, which determines the ratio of the longshore transport that is transported along the spit because of diffracting waves. In the advanced model, the value of the coefficient κ, which quantifies the effect of diffraction on the wave conditions determining the cross-shore transport towards the spit, will have a significant influence on the ebb shoal volume. A κ close to one will reduce the ebb shoal volume substantially, whereas a small κ will result in a volume close to the determined equilibrium volume. A small κ will also result in a large amount of sediment bypassing across the inlet. The transport rate in the inlet channel Q_C affects the spit growth negatively and Q_C may even inhibit the spit growth if it becomes large.

References

Data

Survey Department of Sri Lanka (2000), *Map of Chilaw 1:50 000,* SHEET 46 Series A. B. M. P.

Wikramanayake N (2006), *Wave Data from Chilaw 1995-1997,* Colombo

Published Material

Baranasuriya P W (2001), *Hydrographic Investigations for the Design of an Anchorage In a Complex Lagoon Estuary,* A Spatial Odyssey: 42nd Australian Surveyors Congress, 1-12

Camenen, B and Larson, M (2005), *A Bedload Sediment Transport Formula for the Nearshore*, Estuarine, Coastal, and Shelf Science, 63, 249-260.

Cooper J A G (1994), *Sedimentary Processes in the River-Dominated Mvoti Estuary, South Africa,* Geomorphology 9, 271-300, Elsevier Science B.V., Amsterdam

Dean R G (1988), *Sediment Interaction at Modified Coastal Inlets: Processes and Policies,* Hydrodynamics and Sediment Dynamics of Tidal Inlets, 412-439, Springer Verlag, New York

Domroes M and Ranatunge E (1993), *Analysis of Inter-Station Daily Rainfall Correlation during the Southwest Monsoon in the Wet Zone of Sri Lanka*, Geografiska Annaler. Series A, Physical Geography, Vol. 75 no.3, 137-148, Swedish Society for Anthropology and Geography

FitzGerald D M (1988), *Shoreline Erosional-Depositional Processes Associated with Tidal Inlets*, Lecture Notes on Costal and Estuarine Studies Vol. 29, 186-225, Springer-Verlag, New York

Hayes M O (1980), *General Morphology and Sediment Patterns in Tidal Inlets*, Sedimentary Geology 26, 139-156, Elsevier Scientific Publishing Company, Amsterdam

Komar P D (1998), *Beach Processes and Sedimentation – Second Edition*, Prentice-Hall Inc, New Jersey

Kraus N C (1999), *Analytical Model of Spit Evolution at Inlets,* Coastal Sediments '99, 1739-1754

Kraus N C (2002), *Reservoir Model for Calculating Natural Sand Bypassing and Change in Volume of Ebb-Tidal Shoals, Part I: Description*, ERDC/CHL CHETN-IV-39

Kraus N C and Larson M (2001), *Estimation of Suspended Sediment Trapping Ratio for Channel Infilling and Bypassing*, ERDC/CHL CHETN-IV-34

Kraus N C, Larson M and Kriebel D L (1991), *Evaluation of Beach Erosion and Accretion Predictors*, Coastal Sediments, 572-587

Lanka Hydraulic Institute in association with Centre for Water Research, the University of Western Australia (1998), *Investigations for Chilaw Anchorage – Final Report, Section II of III: Field Investigations and Appendix 3: Beach Profiles, Estuary Morphology & Aerial Photographs*

Larson M, Kraus N C and Hanson H (2002), *Simulation of Regional Long Shore Sediment Transport and Coastal Evolution- the "Cascade" Model*, Proceedings 28th Coastal Engineering Conference, 1-13, World Scientific Press

Larson M, Erikson L and Hanson H (2004), *An Analytical Model to Predict Dune Erosion due to Wave Impact*, Coastal Engineering 51, 675-696, Elsevier B.V.

Plunkett R and Ellemor B (2003), *Sri Lanka*, Lonely Planet Publications, 9th Edition

Ranasinghe R and Pattiaratchi C (1997), *Seasonal Closure of Tidal Inlet*, Coastal Dynamics

Ranasinghe R and Pattiaratchi C (1999), *the Seasonal Closure of Tidal Inlets: Wilson Inlet – a Case Study*, Coastal Engineering 37, 37-56, Elsevier Science B.V.

Ranasinghe R, Pattiaratchi C and Masselink G (1999), *A Morphodynamic Model to Simulate the Seasonal Closure of Tidal Inlets*, Costal Engineering 37, 1-36, Elsevier Science B.V.

US Army Corps of Engineers (1984), *Protection Manual Vol. 1,* Fourth Edition, Coastal Engineering Research Center, Washington DC

Walton T L and Adams W D (1976), *Capacity of Inlet Outer Bars to Store Sand*, Coastal Engineering, 1919-1937

Wikramanayake N, Guneratne P P, Fernando M M G S and Ratnayake I (2003), *the Coastal Wave Climate of Sri Lanka: Measurements and Modeling*, COPEDEC VI, Colombo, Sri Lanka

Wikramanayake N and Pattiaratchi C (1999), *Seasonal Changes in a Tidal Inlet Located In a Monsoon Regime*, Coastal Sediments '99, 1463-1477

Özhan E (1998), *Flow Regimes and Dynamic Equilibrium of Morphological Changes at Köycegiz Lake Inlet Turkey*, Coastal Engineering 12, 109-132, Elsevier Science Publishers B.V., Amsterdam

Internet

Department of Meteorology – Sri Lanka (2006-10)
www.meteo.slt.lk/media.html

US Army Corps of Engineering (2006-10), *Coastal Engineering Manual EM 1110-2-1100*
http://chl.erdc.usace.army.mil/chl.aspx?p=s&a=ARTICLES;104

Television

ITN (2006-06-17), Sri Lankan Television News

Oral

Wikramanayake N (2006-07), Colombo, Sri Lanka

Pictures

All pictures and figures: Alexandra Angelbratt and Jon Klüft (2006)

Appendix 1 - Long shore Sediment Transport

Assumptions

Several assumptions were made when calculating the potential longshore sediment transport. If the wave angle at breaking, θ_b, is small, cos θ_b should be close to one. This requirement was fulfilled so the equation for h_b by Larson et al (2002) could be used. The wave angle in deep water, θ_0, is based on the normal to the local shoreline orientation. The shoreline is assumed to stretch in a perfect north-southward direction based on inspection of maps and information from Wikramanayake and Pattaratchi (1999). The value on the coefficient K in the sediment transport rate equation was taken from US Army Corps of Engineers (2006) and it is assumed to be applicable for the conditions in Chilaw.

Theory

The wavelength under deepwater conditions, L_0, can be expressed as:

$$L_0 = \frac{gT_s^{\,2}}{2\pi} \qquad (21)$$

where T_s is the significant wave period and g represents the acceleration of gravity (9,81 m/s^2) (US Army Corps of Engineering, 2006).

When solving for the water depth at breaking, h_b, the significant wave height, H_{0s}, and wave angle, θ_0, (with respect to the local shoreline) in deep water will be used. The breaker depth ration γ_b is the wave height, H_b, divided by the water depth, h_b, at breaking, in this case taken as γ_b=0.78 (Larson et al., 2002). The depth at breacking is given by:

$$h_b = \left(\left(\frac{H_{0s}}{L_0} \right)^2 \frac{\cos\theta_0}{\gamma_b^{\,2} 2\sqrt{2\pi}} \right)^{2/5} L_0 \qquad (22)$$

The wave angle at the breaking point θ_b, with respect to the local shoreline is:

$$\theta_b = \arcsin\left(\sqrt{2\pi} \sin\theta_0 \sqrt{\frac{h_b}{L_0}} \right) \qquad (23)$$

The volumetric transport rate, Q_l (m^3/s), is calculated from the wave properties at the break point according to:

$$Q_l = K\left(\frac{\rho\sqrt{g}}{16\sqrt{\gamma_b}(\rho_s - \rho)(1-n)}\right)H_b^{5/2}\sin(2\theta_b) \qquad (24)$$

where ρ is the density for water and ρ_s the density for the sediment. Typical values for ρ and ρ_s are 1024 kg/m^3 for salt water and 2650 kg/m^3 for quartz sand, respectively. The coefficient, K, using the significant wave height, is in this case taken as 0.39 based on the Coastal Engineering Manual and n is a pore-space factor with a typical value of 0.4 (US Army Corps of Engineering, 2006).

Results

The calculated potential amount of sediment transported along the coast during the south-west monsoon based on wave data from 1996 is presented in Figure 28. A positive value represents a northward sediment transport while a negative value shows the reverse transport direction. The period between days 68 and 87, with constant sediment flow, represent average wave conditions for the studied period since wave data from this period is missing.

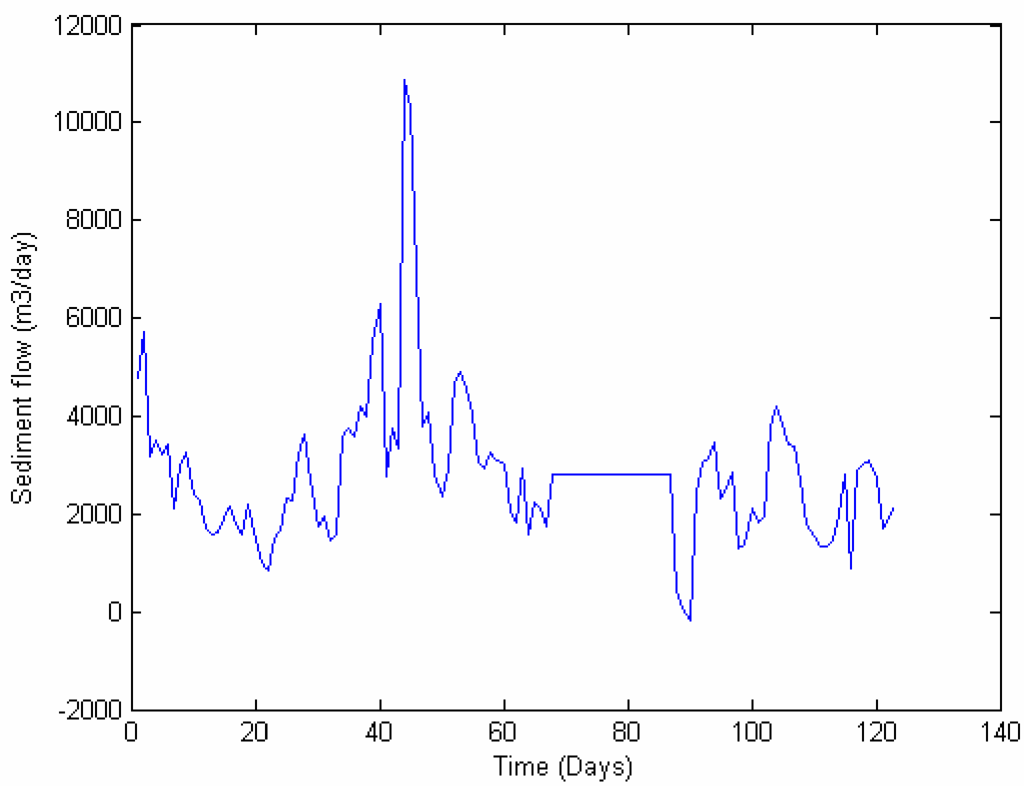

Figure 28: Potential longshore sediment transport during the south-west monsoon

The total potential longshore sediment transport is 350,000 m^3 sediment during the south-west monsoon, in this case from the 1st of May to the 31st of August. This results in an average north-directed sediment transport of approximately 2,800 m^3 per day. The reef beach equilibrium volume, estimated to be 70,000 m^3, is rather small compared to the total potential sediment transport and a lot of the transported sediment will be bypassed to the Chilaw inlet.

Appendix 2 - Depth of Closure

Theory

The depth of closure is calculated according to US Army Corps of Engineering (2006):

$$H_e = \overline{H} + 5.6\sigma_H \quad (25)$$

$$h_c = 1.57H_e \quad (26)$$

where H_e is the effective significant wave height, $\overline{H}$ and σ_H are the average and standard deviation of the significant wave height, respectively, and h_c is the depth of closure (US Army Corps of Engineering, 2006). The average height and standard deviation was estimated from the significant wave height data in MATLAB.

Results

A depth of closure of 4.5 m was obtained.

Appendix 3 - Sediment Transport from Reef Dune

Theory

The sediment transport from the dune to the reef beach is estimated as (Larson et al., 2004):

$$Q_D = 4C_D \frac{\left(R - z_R\right)^2}{T} L_R \qquad R > z_R \tag{27}$$

where C_D is an empirical coefficient, R the runup height, z_R the elevation of the reef above mean sea level, T wave period, and L_R the length of the reef. Transport from the sediment deposit on top of the reef only occurs if the runup height exceeds the top of the reef, that is, $R>z_R$ ($R<z_R$ yields $Q_D=0$). The runup height is computed from the formula:

$$R = 0.158\sqrt{H_o L_o} \tag{28}$$

where H is wave height (root-mean-square height for random waves; $H = H_s / \sqrt{2}$, where H_s is the significant wave height), L wavelength, and subscript o denotes deepwater conditions.

Larson et al. (2004) provided suitable values on C_D, but in the present case this coefficient may be determined by calibration against measurements. From April to August 1996 a certain amount of sand (ΔV_D) was supplied from the dune to the reef beach. The sand transport from the dune deposit may be estimated from Equation 27 for every wave measurement in the time series from April to August. The coefficient C_D is then adjusted so the total calculated volume agrees with the measured volume. Thus, C_D is given by the following expression:

$$C_D = \frac{\Delta V_D}{4L_R \int_0^{t_D} \frac{\left(R - z_R\right)^2}{T} dt} \approx \frac{\Delta V_D}{4L_R \sum_{i=1}^{N} \frac{\left(R_i - z_R\right)^2}{T_i} \Delta t_i} \tag{29}$$

where t_D is the time period during which ΔV_D was supplied to the reef beach, N the number of time steps in the wave time series, and Δt_i the duration of time step i

$(t_D = \sum_{i=1}^{N} \Delta t_i)$.

Results

A value of 0.0201 was obtained for C_D and that gives a Q_D variation in time plotted in Figure 29. The total flow from the reef dune during the south-west monsoon is 80 000 m^3 which gives a daily average of 650 m^3.

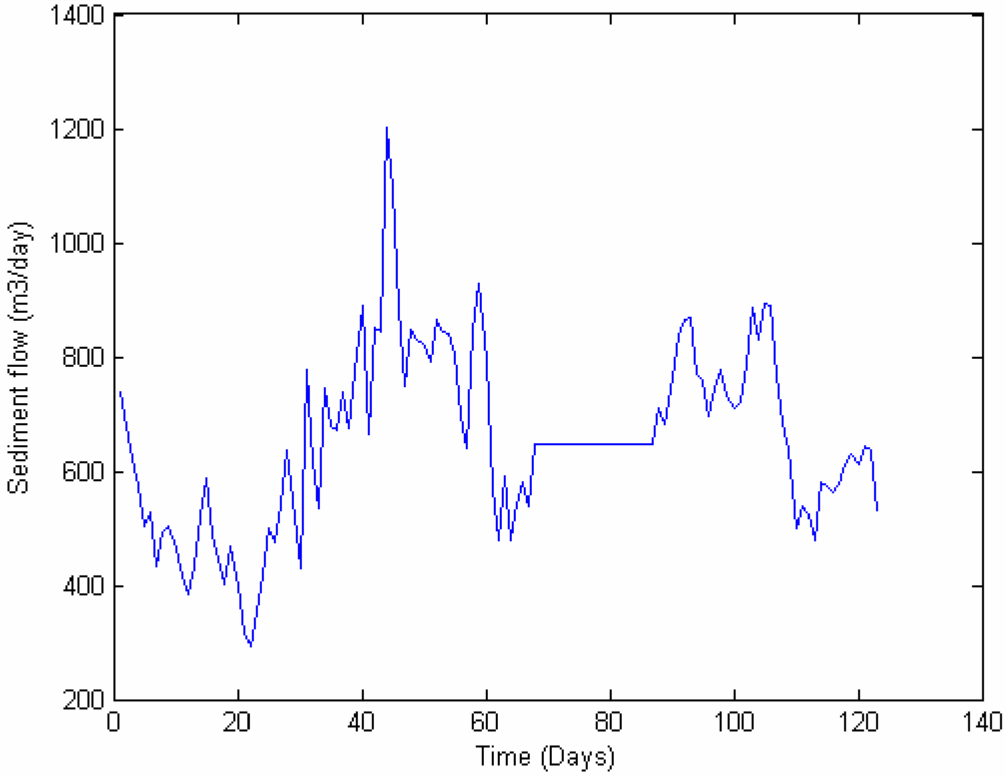

Figure 29: Sediment transport from the reef dune as a function of time

Appendix 4 - Sediment Loss from Ebb Shoal

Theory

The cross-shore sediment transport was calculated by the following heuristic transport formula:

$$Q_E = \frac{\xi}{\xi_{cr}}\left(1 - \frac{\xi}{\xi_{cr}}\right)\frac{V_E}{T_E} \quad (30)$$

where ξ_{cr}=3 and T_E (T_E=10) is an empirical parameter representing the response time scale of the cross-shore sediment exchange and:

$$\xi = \frac{\kappa H_{so}}{wT} \quad (31)$$

in which κ is an empirical coefficient between 0 and 1 that quantifies the influence of diffraction (it is assumed that H_{so} is the wave height measured in the ocean). Equation 30 gives Q_E=0 for H_s=0 and for $\xi=\xi_{cr}$, in agreement with the requirements for the cross-shore exchange model. It is expected that Equation 30 might not be suitable for very large values on ξ, but in the present case the emphasis is on the onshore transport for which these values are below 3.

Results

The coefficient κ was set to 0.3 and that gave the resulting Q_E as seen in Figure 30. Positive values on the sediment flow means that onshore movement will occur, e.g., sediment will move towards the spit. Negative values represent offshore sediment transport from the ebb shoal to the sea.

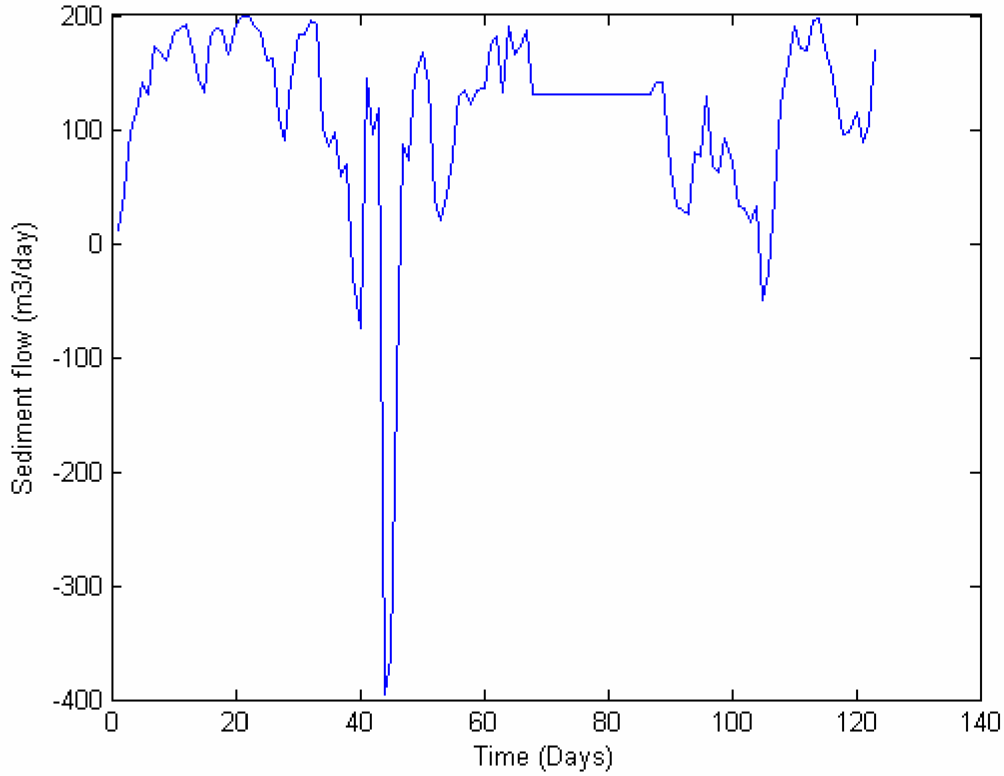

Figure 30: Sediment loss from ebb shoal

Appendix 5 - Sediment Eroding from Spit

Theory

The tidal prism (V_p) of Chilaw lagoon is estimated to be approximately 2.5 Mm^3 and using equations proposed by Walton and Adams (1976) the corresponding cross-sectional area (A_c) may be calculated to be about 85 m^2. Assuming that the velocity varies sinusoidally in the channel during a tidal cycle ($U(t) = U_m \sin\left(2\pi t / T_c\right)$, where t is time and T_c the tidal period), the maximum velocity (U_m) is given by:

$$U_m = \frac{V_p \pi}{A_c T_c} \tag{32}$$

This equation yields a maximum velocity of about 2 m/s for conditions at Chilaw, whereas the mean velocity ($\bar{U}$) during ebb (or flood) is given by $\bar{U} = 2U_m / \pi = 1.3$ m/s.

In order to compute a representative sediment transport in the inlet channel, bed load was assumed dominant and the formula developed by Camenen and Larson (2005) was employed:

$$\Phi = a\theta_c^{3/2} \exp\left(-b\frac{\theta_{cr}}{\theta_c}\right) \tag{33}$$

in which a (=12) and b (=4.5) are coefficients, and the dimensionless transport rate and the current Shields number are defined as, respectively:

$$\Phi = \frac{q_b}{\sqrt{(s-1)gd_{50}^3}} \tag{34}$$

$$\theta_c = \frac{\tau_c}{(\rho_s - \rho)gd_{50}} = \frac{1}{2}\frac{f_c U_c^2}{(s-1)gd_{50}} \tag{35}$$

where q_b is the bedload transport, s the relative density (ρ_s/ρ), g the acceleration of gravity, d_{50} the median grain size, ρ_s the sediment density, ρ the water density, τ_c is the current shear stress ($\tau_c = 0.5 f_c \rho U_c^2$), f_c the current friction factor, and U_c the current velocity. The subscript c denotes current and *cr* critical conditions for incipient motion. For the grain size and water depth at Chilaw the friction factor should be around 0.002, and this value was employed in the present calculations.

The mean transport rate during the ebb (or flood) cycle may be written:

$$\overline{\Phi} = \frac{2}{T_c} \int_0^{T_c/2} a\theta_c^{3/2} \exp\left(-b \frac{\theta_{cr}}{\theta_c} \right) dt \qquad (36)$$

The integral in Equation 36 may be solved by substituting in the sinusoidal velocity variation (Equation 35) and using the shear stress based on the maximum velocity in the exponential term that characterizes the initiation of motion. The critical shear stress was estimated to 0.18 N/m^2 and the maximum shear stress to 4 N/m^2. Substituting in relevant values for Chilaw after integration of Equation 36 gives a transported volume of about 2 m^3/m during a tidal cycle. Since the tide is semi-diurnal there will be two cycles per day, so about 4 m^3/m is transported every day (in the ebb and flood flow combined).

Results

Assuming a representative inlet width of 40 m and correcting for the porosity yields a typical transport rate on the order of 200 m^3/day. This transport rate was employed as a rough estimate in the model simulations. A more sophisticated modeling approach would take into account the variation in the inlet cross-sectional area depending on the balance between the longshore sediment transport and the transport in the inlet channel.